EFFECT OF Fe, Sr AND Mn ON THE MICROSTRUCTURE AND MECHANICAL PERFORMANCE OF SECONDARY CAST Al-Si-Cu-Mg ALLOYS FOR CYLINDER HEAD APPLICATIONS

GAUDENCE NYIRANZEYIMANA

MASTER OF SCIENCE

(Mechanical Engineering)

JOMO KENYATTAUNIVERSITY OF AGRICULTURE AND TECHNOLOGY

2017

Effect of Fe, Sr and Mn on the Microstructure and Mechanical Performance of Secondary Cast Al-Si-Cu-Mg Alloys for Cylinder Head Applications

Gaudence Nyiranzeyimana

A thesis submitted in partial fulfillment of the requirement for the Degree of Master of Science in Mechanical Engineering in the Jomo Kenyatta University of Agriculture and Technology

2017

DECLARATION

This thesis is my original work and has not been presented for a degree in any other university.

Signature: ..... Date.....

Gaudence Nyiranzeyimana

This thesis has been submitted for examination with our approval as the University Supervisors:

Signature: ...  …Date.....

Dr. B. R. Mose

JKUAT, Kenya

Signature: ..... Date.....

Dr. T. O. Mbuya

UoN, Kenya

DEDICATION

To my loving husband, Dieudonné Ruzigamanzi and my parents, Berckmas and Liberée

ACKNOWLEDGEMENTS

I thank the Almighty God for protecting me from the start to the end of this research. I would like to give my thanks to my supervisors, Dr. T.O. Mbuya and Dr. R. B. Mose, for guiding and encouraging me to complete this thesis.

I would like to acknowledge the support from Mobility to Enhance Training of Engineering Graduates in Africa (METEGA) in this research. I would also like to appreciate Regional Universities Forum for Capacity Building in Agriculture (RU-FORUM) for funding this research. I would like to acknowledge Jomo Kenyatta University of Agriculture and Technology for sponsoring this work.

I would like to express my acknowledgement to Mr. Njue for his help, guidance and patience with microscopy experiments. I would like to acknowledge the support and advice of Dr. Eng. Hiram Ndiritu. I would like to appreciate my colleagues Kakande Lawrence, Anold Taremwa, Quarty Gideon, Muchemi and Yin Edward for their support, encouragements and help in formatting and organizing this thesis. I would also like to appreciate Mr. Ngigi for his helping during the experiments.

Finally, my sincere gratitude is given to my husband, Dieudonné Ruzigamanzi, my parents, Berckmas and Liberée, my brother, Emmanuel, and my sister, Jeanette, for their understanding, continuous encouragement, care, and full love.

TABLE OF CONTENT

LIST OF TABLES

LIST OF FIGURES

LIST OF ABBREVIATION

BA Base Alloy

CO_2 Carbon Dioxide

Cu Copper

Fe Iron

FCG Fatigue crack growth

H. T Heat treated

EDS Energy Dispersive X-ray Spectroscopy

Mn Manganese

O Oxygen

OM Optical Microscopy

SDAS Secondary Dentrite Arm Spacing

SEM Scanning Electron Microscopy

Sr Strontium

S-N Stress amplitude vs number of cycles to failure

UTS Ultimate Tensile Strength

UoN University of Nairobi

SYMBOLS

d	Neck diameter
I	Moment of Inertia
L	Distance from the load to the neck of specimen
$\mathbf{L_f}$	Final gauge length [mm]
$\mathbf{L_i}$	Initial gauge length [mm]
µm	Micro-meter
M	Bending Moment
P	Applied load
r	Neck radius
$\boldsymbol{\sigma_b}$	Fatigue Strength

ABSTRACT

Cast aluminium alloys have many uses such as in the automotive industry as well as for manufacturing purposes like in construction industry to fabricate windows and door frames. These alloys are important because they are light and as such reduce vehicle weight; they have good fluidity and are corrosion resistant. However, the microstructure and mechanical properties of recycled aluminum alloy are still unpredictable. This is mainly due to problems associated with controlling the chemical composition of the recycled aluminium alloys since the chemical compositions of the various scrap inputs are different. Solidification after casting defines the mechanical properties of cast alloy through the resulting microstructure. The main objective of this research is to develop a high performance recycled aluminium alloy for automotive cylinder head applications. Previous study has mainly focused on the development of recycle-friendly alloys for automotive cylinder head applications. The mechanical properties that were carried out recommended reusing directly the cylinder head scrap. The present research focuses on the effect of minor elements additions such as Sr, Fe and Mn on the microstructure and fatigue performance of recycled Al-Si alloy for cylinder head applications. The alloy used in this study was obtained by melting different scrap cylinder heads from small vehicles and then was tested to predict their fatigue performance after element additions in heat treated and as cast conditions. The specimens for the fatigue tests and the microstructural analysis as well as tensile

tests were machined from the resulting alloys. An Optical Microscopy (OM) and Scanning Electron Microscopy with Energy Dispersive X-ray Spectroscopy (SEM/EDS) were used to investigate the microstructural characterization. The tensile test specimens were machined according to the ASTM B557M standard. Fatigue life performance was investigated at room temperature using S-N fatigue data. Constant amplitude, fully reversed fatigue tests under a stress ratio of R = -1 was carried out using a rotating bending machine. The microstructure features of base alloy consisted mainly of a structure with primary Al-matrix, coarse acicular Si particles and intermetallic phases such as Al_2Cu and AlCuNi. When 0.02%Sr was added to the base alloy, coarse acicular Si particles were modified to a fine fibrous form. With addition of 0.38%Fe, results in the formation of large eutectic silicon particles and Fe rich intermetallic. Moreover, when 0.45%Mn was added in combination with 0.9%Fe, the Al_2Cu, and α-AlFeMnSi with Chinese script morphology were identified. It is noticed that after T6 heat treatment, the Si particles are seen to spheroidize and fragment while the Al_2Cu phases dissolve completely. These changes lead to improved mechanical performance of the alloy. The results also showed that the strontium addition has the highest average UTS in both as cast and after T6 heat treatment condition. The ductility of the alloys decreased after T6 heat treatment. The highest fatigue lives in the as cast alloy were observed in the base alloy with strontium. After T6 heat treatment, the fatigue performance of base alloy with iron and manganese increased while the fatigue life of base alloy and with strontium decrease. These results obtained from this study

can be used by automotive powertrain component manufacturers to produce high quality engine parts using secondary Al-Si alloys.

CHAPTER ONE

INTRODUCTION

1.1 Background

The need for aluminium and aluminium products is increasing because aluminium alloys offer excellent corrosion resistance with good strength and low density compared to steel. Aluminium, when used in automobile applications, saves much more energy through component weight reduction and reduces greenhouse gas emissions since producing aluminium by recycling creates only 5% of CO_2 that is generated during primary production [1]. The main application of aluminium in the automotive industry is in fabrication of cylinder heads. In this application, the major advantage of aluminium besides its low density is its low coefficient of thermal expansion, which allows combustion heat to be extracted more rapidly [2,3,4].

Aluminium alloys such as 319.0, 356.0, 355.0, 354.0 or A380.0 families are commonly used in casting cylinder heads. An increase in the use of aluminium alloy products coupled with the ease with which aluminium alloys can be recycled has led to an expansion of the cast secondary aluminium alloy industry worldwide. It is visualized that the use of recycled cast aluminium will continue to increase and hence the need for a complete understanding of its properties in comparison with primary aluminium alloy products as well as other engineering materials. A secondary aluminium product is

becoming an important component of aluminium production and is attractive because of its economic and environmental benefits [1].

Increasing recycled metal availability is a positive trend as secondary aluminium produced from recycled metal requires only about 2.8 kWh/kg of metal to produce while primary aluminium production requires about 45 kWh/kg of metal. Therefore melting 1 kg of recycled metal saves almost 95% of the energy needed to produce primary aluminium from ore. This also leads to a reduction in pollution and greenhouse emissions arising from mining process, ore refining and melting. Increasing the use of recycled metal is also quite important from an ecological standpoint, since producing aluminium by recycling creates only about 5% CO_2 that is generated by primary production [5].

However, the castability, microstructure and mechanical performance of these recycled alloys are more susceptible to casting defects. This is due to the different mix of trace elements and high levels impurities elements as well as varying degrees of minor elements. This will result in lower mechanical properties and unreliability of the cast aluminium alloys [6].

It has been reported that the increasing the amount of iron from a critical percentage may lead to the formation of detrimental intermetallic phases such as β-phases. This type of intermetallic has the most significant effect on the mechanical properties of Al-Si alloys. It especially decreases ductility because this compound tends to form thin platelets which are very brittle and have substantially low bond strength with the matrix [7]. It

has also been indicated that that cracks initiate at the intermetallic particles in absence of casting porosity. Therefore, the presence of intermetallic phases such as these β-phases in Al-Si alloys may result in negative mechanical properties.

To eliminate the effects of intermetallic phases and enhance the performance of Al-Si alloys, several researchers have observed that, the microstructure can be modified and mechanical properties can be improved by alloying and heat treatment. For example Tash et al [8] observed that additions of small amounts of alloying elements change the morphology of intermetallic phases. Tash et al [8] indicated that the surface or volume fraction of Fe-intermetallics was observed to be higher in the unmodified alloys than the modified ones, as a result of the fragmentation and dissolution of the intermetallics due to the presence of Sr in the modified alloys. This leads to improved mechanical properties of cast Al-Si alloys.

Addition of manganese, may reduce the intensity of negative effect of iron by altering the β-phases into Chinese script. This leads to improvement of the fatigue strength and the impact properties of aluminum alloys [9].

Zeru et al [10] observed that the addition of 0.02% Sr to Al-Si cast alloy for cylinder heads reduced the fluidity by 5.2%. The increase of iron content of the base alloy to 0.38% Fe decreased the fluidity by 21.9%. This is attributed to the formation of intermetallic phases that blocks the interdendritic channels which are responsible for compensating for solidification shrinkage. However, combined addition of 0.9% Fe and

0.45% Mn was observed to reduce the fluidity by 12.1%. It is necessary to develop further analysis based on these four alloys tested. This research is focused on the effect of specific minor elements on the microstructure, tensile and fatigue performance of this alloy.

Fatigue life of cast aluminium alloys is determined by the maximum flaw size. The larger the casting flaw, the lower the fatigue strength and the shorter the fatigue life [11]. Fatigue is a crucial mode of failure which refers to a condition whereby material cracks or fails because of repeated (cyclic) stresses applied below its ultimate strength. When a structure is loaded repeatedly, a crack will be nucleated on a microscopically small scale. This crack grows and then complete failure of the specimen finally occurs. The whole process constitutes the fatigue life of the component. When a new material is manufactured, it is very important to know its fatigue life [12].

One of the important goals in the fatigue process study is the forecast of the fatigue life of a structure or machine component subjected to a given stress [13]. Cast aluminium alloys have been extensively used in the production of critical automotive components, including engine blocks and cylinder heads. Increasing use of aluminium castings in automotive as well as aerospace industries can be realized by paying great attention to fatigue properties of cast aluminium components [11].

1.2 Problem Statement

Aluminum castings are good candidates for automotive, electronic, aeronautic, sport equipment and other high performance products. The microstructure and mechanical properties of recycled aluminum alloy are still unpredictable. This is mainly due to problems associated with controlling the chemical composition of the recycled aluminium alloys since the chemical compositions of the various scrap inputs are different. There is a need to reduce compositional effects on castability of aluminium by increasing the number of alloys with specific composition. This will allow direct reuse of recycled Al-Si alloy which requires limitation of minor and major alloying elements as well as impurity elements. It has been found that secondary aluminium alloys for automotive cylinder heads applications obtained by melting different scrap cylinder heads are almost equivalent in terms of alloy chemistry to commercial Al-Si-Cu-Mg based alloys [14]. Previous work has concentrated on the development of recycle-friendly alloys for automotive cylinder head applications where the investigation was done on fluidity and some mechanical properties like hardness and impact toughness. The results obtained allow direct reuse of cylinder head scrap. This research therefore was focused on fatigue, tensile behaviour and their relationships with the microstructure of cast aluminium alloy for selected cylinder head scraps.

1.3 Objectives

1.3.1 General Objective

The overall aim of this research was to study the effect of Fe, Mn, and Sr on the microstructure and mechanical performance of a recycled Al-Si-Cu-Mg alloy for use in automotive engine cylinder heads.

1.3.2 Specific Objectives

The following are the specific objectives:

- To characterize the effect of Fe, Mn and Sr on the microstructure features on a secondary Al-Si-Cu-Mg alloy.
- To characterize the effect of Fe, Mn and Sr on the tensile properties on a secondary Al-Si-Cu-Mg alloy
- To characterize the effect of Fe, Mn and Sr on the fatigue properties on a secondary Al-Si-Cu-Mg alloy

CHAPTER TWO

LITERATURE REVIEW

2.1 Introduction

Recycling of aluminium alloys is beneficial both financially and environmentally and has become a major industry. This is because aluminium alloys can be recycled many times without losing their properties. In addition, huge energy savings are possible since recycling uses only 5% of the energy required to extract and refine new aluminium. Many specialized aluminium alloys have been developed for applications in aviation and automotive industry. Aluminum alloys are used extensively in automobile due to their high strength-to-weight ratio [15]. In the past, most of the engine components were constructed from cast iron, but currently aluminium has replaced cast iron to reduce component weights [16,17]. Since there is need of a wide range of properties in cast aluminium alloys, there have been developments to improve their microstructure, which has direct influence on their mechanical properties.

The physical and mechanical properties of cast Al-Si alloys are significantly influenced by the alloy composition, impurity elements, melt treatments, solidification characteristics, casting defects, and heat treatment as described hereunder.

- Alloying composition: The composition of alloys determines the potential for achieving special physical and mechanical properties. Alloy content is designed to produce characteristics that include castability as well as desired performance capabilities. The interaction of alloying elements is recognized in promoting desired microstructural phases and solid-solution effects for the development of these properties [18]. Several metals can be added to aluminium. Among those regularly added and controlled as alloying elements are strontium, iron, manganese, silicon, copper, magnesium and zinc. Some are used as solid solution strengtheners, while others are added because they form various desirable intermetallic compounds [4]. The presence of alloying elements such as Cu, Fe, Mg, Mn leads to formation intermetallic compounds [19].
- Impurities: The impurity rich phases which impair mechanical properties are frequently found in intergranular or interdendritic regions. While a number of impurity elements can affect mechanical properties, iron is the most common and recognized as the most deleterious, particularly to ductility and toughness [20].
- Cooling rate during and after solidification: The conditions under which solidification takes place determine the structural features that affect the physical and mechanical properties of an alloy.
- Heat treatment: Mechanical properties can be altered by post-solidification heat treatment, including annealing, solution process and precipitation aging.

Modification treatment can improve elongation to failure to a great extent as long as the intermetallic compounds are refined in size.

- Casting defects: The level and type of defects in Al-Si castings depend on the condition of the melt, the manufacturing process and post solidification treatments. Such defects in the castings cause an unfortunate scattering of the mechanical properties and degrade the performance of the component.

Moreover, the fatigue behavior of Al-Si casting alloys is affected by the solidification microstructure characteristics and especially by casting defects such as gas pores, shrinkage pores and oxide films [21]. According to Fintova et al [22] the fatigue behavior depends on size, number and position of pores. However, the deleterious effect of casting defects has also been recognized. Molten metal of aluminum is prone to hydrogen absorption and oxidation; gas porosity and oxide inclusions are inevitably found in aluminum castings. In addition, if the casting is not properly fed, shrinkage porosity results, which is also quite deleterious to fatigue properties. The fatigue failure initiates from the various microstructural features such as either brittle intermetallic particles or eutectic Si particles in absence of porosities and inclusions [23,24].

This section presents a review of cast aluminium alloy, effect of alloying elements on microstructure and mechanical properties of Al-Si cast alloys, effect of cooling rate and heat treatment on mechanical properties of Al-Si alloys, factors controlling fatigue damage and finally, life distribution of these alloys.

2.2 Cast Aluminium-Silicon Alloys

Aluminium alloys with Si as the major alloying element form a class of material providing the most significant part of all casting manufactured materials. These alloys have a wide range of applications in the automotive and aerospace industries due to an excellent combination of castability and mechanical properties, as well as good corrosion resistance and and wear resistance. Depending on the Si concentration in weight percent (wt. %), the Al-Si alloy systems fall into three major categories: hypoeutectic (<12%Si), eutectic (12-13%Si) and hypereutectic (14-25%Si). The most common of these alloys belong to the hypoeutectic group in which the silicon content is between 5-12 wt% [25].

2.3 Microstructure of Cast Aluminium Alloys

The microstructure of cast Al-Si-Cu/Mg alloys is typically determined by three components, the proportions of which are governed by the alloy composition and solidification rate. Two major microstructural components, namely primary α-aluminium solid solution phase and Al-Si eutectic. The third component of microstructure is intermetallics and these arise from excess amount of Mg, Cu, Fe and Mn that cannot be contained in α-Al solid solution phase. The presence of Cu, Mg and Fe in the alloy leads to formation of various intermetallic compounds in the microstructure of the alloy. The most common intermetallic phases are Al_2Cu, Mg_2Si, αAl_{12} $(Fe,Mn)_3Si_2$ and β-Al_5FeSi. The intermetallics phase adopt various morphologies

and form at various times, prior to, during or after Al-Si eutectic formation period and can significantly affect mechanical properties of the alloys [26].

Microstructure and mechanical properties of cast Al-Si alloys are significantly influenced by the casting conditions such as solidification rate, melt treatment and the casting process [4]. Hence, it is important to control the microstructure of these alloys during the final stages of solidification since it is during these stages that different microstructural phases form [24].

Figure 2.1 shows an example of the structure of hypoeutectic $AlSi_6Cu_4$ cast alloy which is composed by α-matrix, eutectic (Si particles in -matrix) and many Cu- and Fe-rich intermetallic phases.

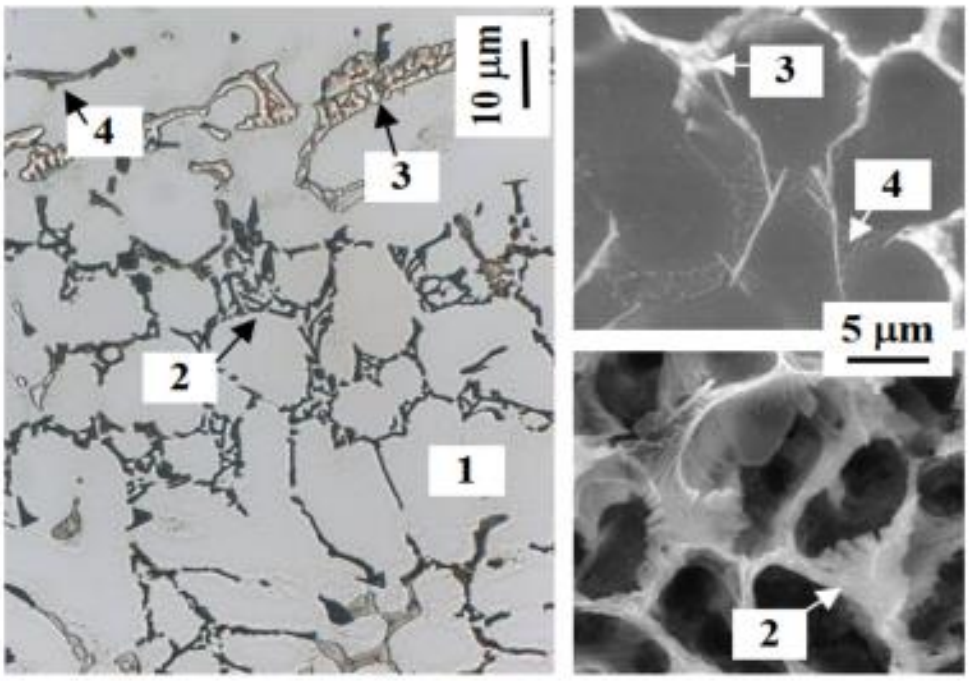

Figure 2.1: Optical and SEM Microstructure of $AlSi_6Cu_4$ alloy, etch. 0.5 HF (1 -α-matrix, 2 eutectic Si, 3 - Cu-phases, 4 - Fe-phases) [27]

2.4 Effects of Some Alloying Elements on Cast Aluminium Alloys

Solidification after casting determines the mechanical properties of cast alloy through the resulting microstructure. The best way to improve mechanical properties of Al-Si alloys is via modification. Since the Al-Si eutectic consists of a hard, brittle Si phase in a softer Al matrix, fine eutectic silicon along with fine primary aluminum grains improves mechanical properties and ductility [28,29]. Modification describes the method in which inoculants in the form of master alloys are added to an Al melt in order to raise the

formation of a fine and fibrous eutectic Si structure during the solidification process [29].

The microstructure can be modified and mechanical properties can be improved by alloying elements. Consequently, alloying elements are selected based on their effect and suitability [18]. Alloying elements can form fine precipitates, refine grain size, modify silicon phase morphology, and reduce the effects of defects and thus can usually increase both fatigue and wear resistance [30].

2.4.1 Iron

Iron improves hot-tear resistance and decreases the tendency for die sticking or soldering in die casting. Increasing iron content is accompanied by substantially decreased ductility [31]. Iron reacts to form a number of intermetallic phases, the most common of which are $FeAl_3$, $FeMnAl_6$, and AlFeSi. These essentially insoluble phases are responsible for improvements in strength, especially at elevated temperature, but also the embrittlement of the microstructure. As the fraction of insoluble phases increases with increased iron content, casting considerations such as feeding characteristics are adversely affected. In concentrations of above 0.7wt percent iron has detrimental effects to mechanical properties and manganese is often used to counter its effects [32].

However, excess amount of iron in the alloy leads to the formation of β phase such as β-$FeAl_5$ that can increase porosity in the casting due to the blocking of metal feeding during solidification shrinkage [7]. In addition, β - Fe intermetallic phase is brittle and

may act as stress raisers during service of a material and affects negatively mechanical properties of alloy [7]. Khraisat [33] studied strengthening aluminium scrap by alloying with iron. The analysis of the results showed that the effect of the 1% addition of iron to aluminium scraps has a positive effect on the mechanical properties of the aluminium scraps i.e ultimate tensile strength and elongation to fracture. This was attributed to the precipitation of intermetallic compound on the grain boundaries of aluminium. Increasing the amount of iron to above 1% deteriorates the mechanical properties except for hardness. This is due to increase in the amount of hard inter-metallic phases in the microstructure.

2.4.2 Strontium

Strontium modifies the aluminium-silicon eutectic. Effective modification can be achieved at very low addition levels; lower concentrations are effective with higher solidification rates. Higher addition levels are associated with casting porosity. Degassing efficiency may also be adversely affected at higher strontium levels. Sr modifier added to the melt, has been observed to increase amount of porosity in the casting [34].

The eutectic silicon phase is needle-shape like. In some mechanical properties test, the fracture initiates readily at these silicon particles, because these silicon needles are very brittle. In order to improve properties, strontium is used as modifiers in Al-Si cast alloys. Generally, 0.02% strontium is used. It is necessary to modify the needle silicon phase into a spherical morphology and the needle β phase into Chinese script-shape α phase in

319 alloys. The addition of Sr refines the morphology of the α-Fe Chinese script phase which in turn contributes to a slight improvement in ductility [31].

According to [35] Sr is a very effective element to change the size, amount and morphology of the intermetallic compounds. This is because Sr successfully modified the large, highly branched β-needle-like phase (β-$FeAl_5Si$) into the individual, less-branched and finer one.

2.4.3 Manganese

Normally considered an impurity in casting compositions, manganese is controlled to low levels in most gravity cast compositions. Manganese is an important element in work-hardened wrought alloys through which secondary foundry compositions may contain higher manganese levels. In the absence of work hardening, manganese offers significant benefits in cast aluminium alloys. Recently, it has been reported that as the manganese content increases over 0.5 wt. % in aluminium alloys, both yield strength and ultimate tensile strength increase significantly without decreasing ductility. Adding manganese to aluminium alloys enhances the tensile strength as well as significantly improves low-cycle fatigue resistance. Corrosion resistance is also improved by the addition of manganese [18].

2.4.4 Iron and Manganese

Iron and manganese have different effects on the microstructure and mechanical properties of Al-Si cast alloy. In addition, manganese and iron form ternary compounds

with aluminium and silicon. Iron addition to Al-Si alloys reduces the number of nucleation events of the Al-Si eutectic whereas Mn addition increases the number of nucleation events in Fe-containing alloys. Iron is a well known impurity element in aluminium alloys while Mn is usually added to neutralize the effect of Fe [7]. Fe enters the intermetallic phases regardless of its concentration in the alloy.

Several researchers [18,20,36] studied the effect of Fe on the microstructures and properties of cast Al-Si alloys. It has been observed that the needle-like β-Fe phase is detrimental to the mechanical properties because it acts as stress raisers. Further, large Fe-rich needles tend to block the flow of liquid metal through the feeding channels and may cause porosity. Mn usually is present in the Fe-containing phases and often substitutes part of Fe. Mn addition is used to decrease the detrimental effects of the Fe-rich phases by replacing it with the less detrimental Chinese script α-Fe phase, resulting in the improvement of mechanical properties. Addition of high amount of Mn were reported to create porosity in alloy [37].

Ashtari et al [35] studied the influence of Sr and Mn additions on intermetallic compound morphologies in Al-Si-Cu-Fe Cast Alloys. The results showed that in the absence of Mn, no Chinese scripts were formed. Combined addition of Sr and Mn has been found to be more effective than the Sr addition to modify the needle-like β-$FeAl_5Si$ phase to shorter, more separated ones and changing the morphology to the Chinese script type.

Fang et al [36] reported that the harmful effect of Fe can be eliminated by the removal of large needle-shaped primary βAlFeSi compound. Chemically, this could be achieved by limiting the maximum level of Fe impurity, or by alloying with elements such as Mn to replace the monoclinic βAlFeSi with a cubic αAlFeMnSi phase. The critical Mn/Fe ratio for the elimination of the primary βAlFeSi varies with alloy composition.

Figure 2.2 shows an example of the microstructure of unmodified Al-Si cast alloys comprising of large β intermetallic compound in an alloy with 1.4%Fe. In Figure 2.3 the microstructure of the alloy modified by iron and manganese addition is shown. Most β phase transformed to α phase in the form of Chinese script. It has observed that increasing Fe and Mn increased volume percentage of α intermetallic phase [38].

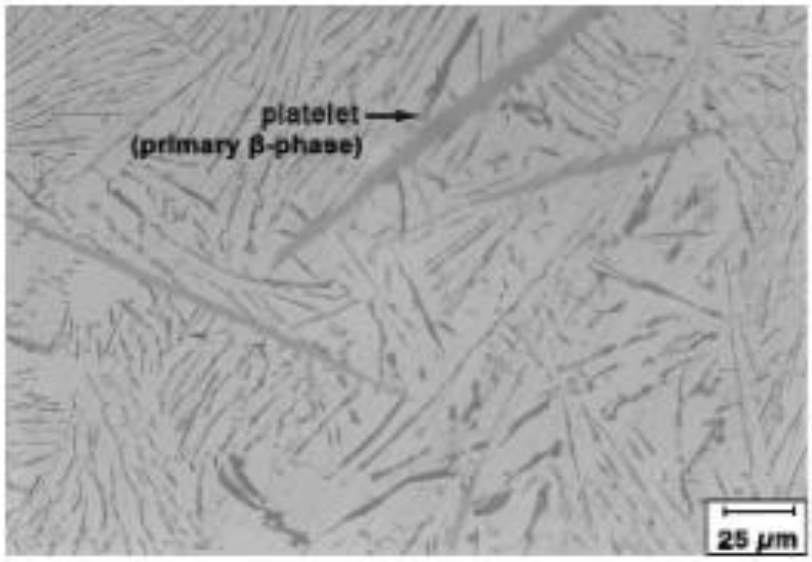

Figure 2.2: Microstructure of unmodified alloy containing 1.4 per cent Fe showing β-Fe platelets surrounded by unmodified eutectic silicon particles [38]

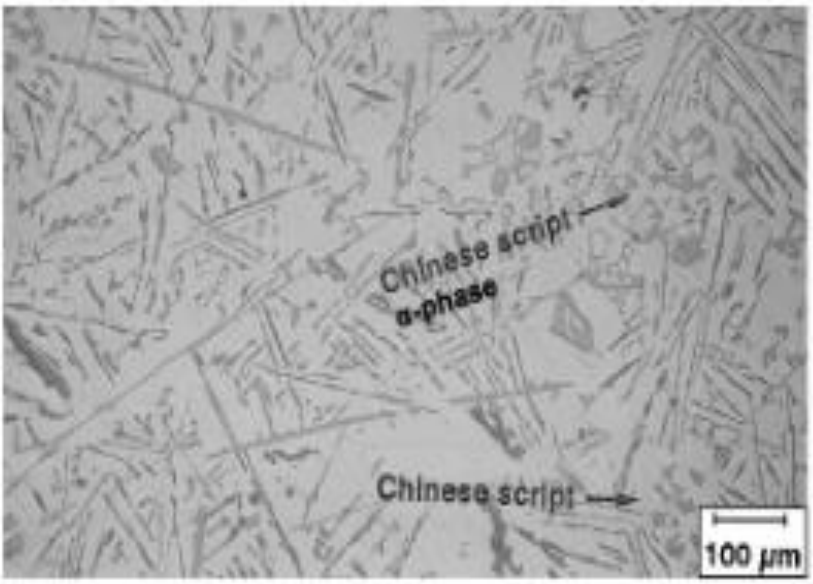

Figure 2.3: Microstructure of the Mn-modified alloy containing 1.4 per cent Fe showing α -Fe [38]

2.4.5 Magnesium

Magnesium improves strengthening and work hardening characteristic of aluminium silicon alloy. It can also enhance good corrosion resistance and weldability or high machinability of alloy [18,39], using Mg alloys results in a 22% to 70% weight reduction in Al-Si alloys.

2.4.6 Copper

Copper has a great impact on the strength and hardness of aluminium casting alloys, both heat treated and non-heat treated and at both ambient and elevated service temperature. It improves the machinability of the alloy by increasing matrix hardness [18]. The addition of small amounts of Cu, between 0.35 and 1.0 wt%, showed a beneficial effect on the hardness [40].

Djurdjevic [41] investigated the effect of major alloying elements on the size of the secondary dendrite arm spacing in the as-cast Al-Si-Cu alloys. Experiments have been carried out to observe the effect of silicon additions between 1.3 and 9.7 wt. % and copper additions between 0.37 and 4.7 wt.% on the size of the secondary dendrite arm spacing (SDAS) in Al-Si-Cu alloys. It was found that addition of silicon and copper reduce slightly the size of SDAS compared to the effect of the cooling rate, but still not so insignificant that the influence can be ignored. This decrease in the size of the SDAS

seems to correlate well with a formation of a large volume of dissolved alloys during solidification of the aluminium alloys with high content of silicon and copper.

Abdulsahib [19] studied the mechanical behavior of Al-12wt%Si recycled alloys and observed that the tensile strength, yield strength and Vickers hardness increased with increasing copper content. The elongation and reduction area decreased with increase of copper additions to base alloy.

2.5 Properties of Cast Aluminium Alloys for Cylinder Heads

Almost 100% of all cylinder heads of the current light vehicle production are made from cast aluminium alloys. These alloys have to maintain continuously growing requirements in terms of strength, ductility and heat resistance at elevated temperatures [2]. As reported by Angeloni [42] cylinder heads are subjected to mechanical and thermal tensions that are relatively high during service. During long run times and in case of any failure in cooling and/or lubrication the temperature may reach 300^0C. This temperature variation causes thermal shocks which may generate cracks and/or a wide range of plastic deformation in the regions close to the pistons. Even without considering the thermal shock effects caused by failure, short numbers of start-up and shutdown cycles of engine are considered the main cause of small cracks. This indicates that generation of cracks in cylinder head may be considered as fatigue problem. To increase engine efficiency, the maximum operating temperature of cylinder heads has increased from approximately 170^0C in earlier engines to peak temperatures well above 200^0C in recent engines [43].

The material suitable for this application must therefore have a low thermal expansion coefficient, high tensile and compression strength, high ductility and a high creep resistance at both room and high temperatures [44]. Furthermore, the alloy should have a high thermal conductivity, high castability and machinability. Castability of this alloy exhibits good fluidity, resistance to hot cracking and solidification shrinkage tendencies [45]. This is a good combination of properties to achieve as some of the requirements, allow the cast aluminium alloys for cylinder heads to retain their leading position in the production of aluminium cylinder heads in the near future [2]. Cylinder heads, in particular, have to withstand higher operating temperatures and stress levels [44].

2.6 Effect of Cooling Rate on Microstructure

The casting process, in combination with component design (section thickness) and the geometry of feeders, risers and gates, largely determines the solidification rate obtained within a casting. A faster rate generally leads to the formation of finer structure at the microscopic level, i,e. smaller dendrites, silicon particles, iron containing intermetallics and porosity. A finer microstructure generally gives increased strength and ductility. Aluminium dendrites and eutectic silicon only varied with cooling rate, becoming finer at faster cooling rates [20]. Increasing the solidification rate reduces the size of microstructural features including eutectic silicon and intermetallics. This makes propagation of a crack through the material more difficult thereby increasing elongation in particular but also ultimate tensile strength [20].

According to Kadhim [46] higher cooling rates enhance the strength, hardness and impact resistance for the Al-Si alloys, while the low cooling rates reduces these mechanical properties. The percentage of elongation and the amounts of formed porosity decreased when the cooling rates increased. Kadhim [46] also observed that high cooling rates decrease the amounts of porosities. This is because there is no sufficient time for formation of big amounts of gas porosity or join this porosity with shrinkage porosity and make cavities. So the percentage of porosity is high when the cooling rate low.

The secondary dendrite arm spacing (SDAS) is one of the most important microstructure features of as-cast structure in hypoeutectic aluminum alloys. The size of SDAS depends on cooling rate/solidification time. With shorter solidification time SDAS decreases [47].

According to [48] the SDAS is strictly dependent on the cooling rate. In the highest cooling rate (e.g 1.04°C/s), the SDAS was fine (≈ 26.6μm) and easily visible. For the sample that was cooled with lowest cooling rate (e.g. 0.16°C/s), the SDAS is large (≈ 79.06μm). Kabir et al [49] indicated that the SDAS decreases with increasing pouring temperature due to multiplication of nucleation sites in the superheated liquid melt. The percentage porosity of the cast aluminium alloys decreases with increasing pouring temperatures and is lowest for metal mold at highest pouring temperature. The relationship between SDAS and cooling rate (R) in cast aluminium alloys is as shown in Figure 2.4.

The increasing solidification rates are also useful in maintaining a finer distribution of lamellae relative to the growth of the eutectic particles. The eutectic is more or less uniformly distributed among the grains of the primary phase. It was noticed that the size of dendrites size and interdendritic arm spacing was small in case of gravity die cast specimen than sand cast specimen. This was attributed to faster cooling rate in case of die casting than the sand casting [50]

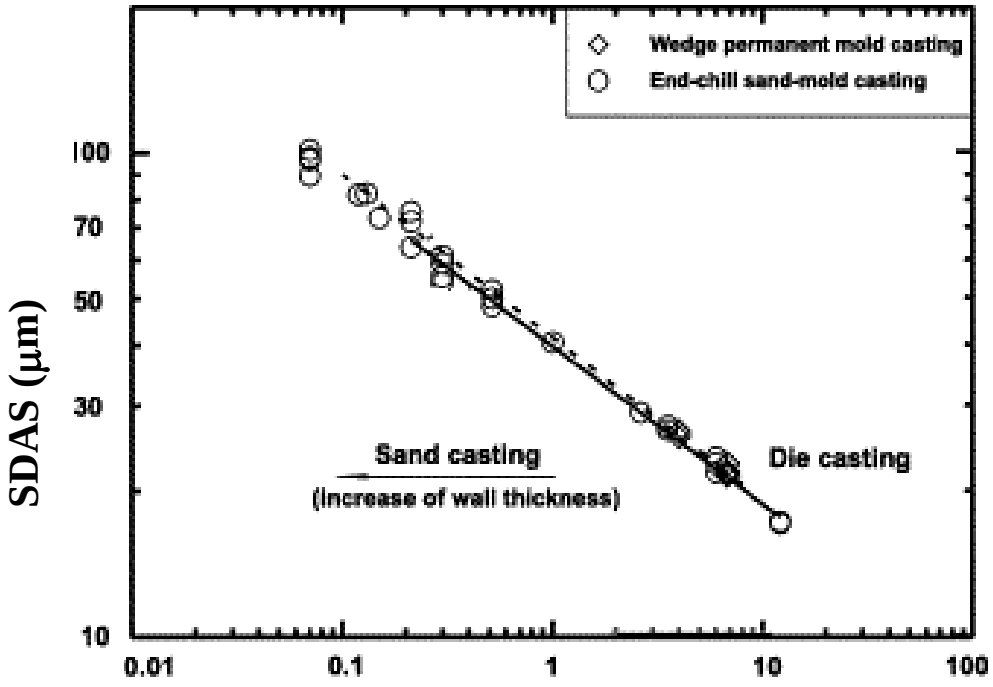

Figure 2.4: Variation of SDAS with cooling rate [47]

2.7 Heat Treatment of Alluminium Alloys

Heat treatment is the process of heating and cooling material to the desired temperature to improve the mechanical properties. The purpose of heat treatment in the aluminium alloys is to maximize the mechanical properties and to modify the microstructure of the alloys. There are several heat treatment processes for aluminium alloys but the most used is T6 Temper due to the resulting good properties [51].

The T6 consists of solution heat treatment and quenching, followed by artificial aging. Solution heat treatment increases ultimate tensile strength (UTS) and ductility, while aging increases yield strength (YS) at the expense of ductility. Solution heat treatment is carried out near the solidus temperature. Generally, depending upon the Cu content, Al-Si-Cu and Al-Si-Cu-Mg alloys are solutionized between 480^0C and 525^0C, which is less than the solutionizing temperature (540^0C) for Al-Si-Mg alloys [52].

According to rules of conventional solution treatment, the solution heat treatment temperature of Al-Si-Cu and Al-Si-Cu-Mg alloys is regulated to 495^0C; this is to avoid completely the incipient melting of the copper-rich phase. This incipient melting tends to decrease the mechanical properties of the casting. Hence, in the Al-Si-Cu-Mg alloys, high solutionizing treatment temperatures are not used to avoid incipient melting. As expected, with lower solutionizing temperatures, longer solutionizing times are required of above 6 to12 hours [53,54].

Quenching is the cooling process which follows solution heat treatment. In many cases, cold water ($10 - 32^0$C) is commonly used in the quenching of aluminum alloys. However, cold water occasionally produces unacceptable distortion due to high thermal gradients that exist in the part. When this problem exists, the part can be quenched in hot water ($60 - 70^0$C) to decrease these thermal gradients and eliminate the possibility of cracking [55]. Finally, artificial aging of Al-Si alloys in the temperature range of $170 - 210^0$C gives high yield strength while Cu containing alloys show a decrease in yield strength with increasing ageing temperature [53]. Consequently, the T6 heat treatment consists of the following stages:

1. Solution treatment at high temperature, close to the eutectic temperature of the alloys. The purpose of solution treatment is to: homogenize the alloying elements, dissolution of certain intermetallic phases such as Al_2Cu and Mg_2Si and change of the morphology of eutectic silicon.

2. Quenching, usually to room temperature, is done to obtain a supersaturated solid solution of solute atoms and vacancies.

3. Age hardening, to cause precipitation from supersaturated solid solution either at room temperature (natural ageing) or at an elevated temperature (artificial ageing). The T6 heat treatment is illustrated in Figure 2.5 for an Al-Si-Cu alloy as an example. The evolution of the microstructure is shown; from (1) atoms in solid solution at the solution treatment temperature, through (2) a supersaturated solid solution at room temperature after quench, to (3) precipitates formed at the artificial ageing temperature [52].

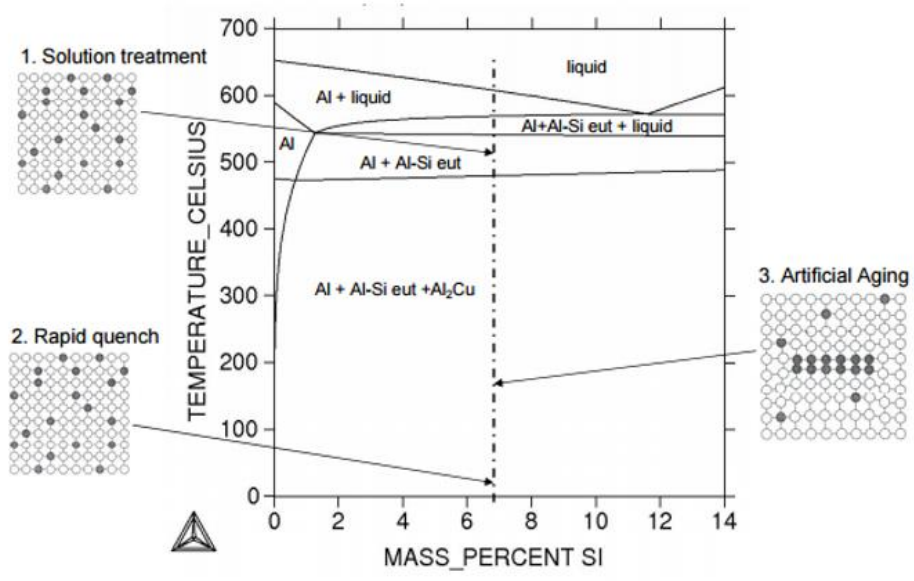

Figure 2.5: The T6 heat treatment process [52]

The changes in the size and morphology of the silicon phase have a significant influence on the mechanical properties of the alloy. It has been proposed that the granulation or spheroidization process of silicon particles through heat treatment takes place in two stages such as fragmentation or dissolution of the eutectic silicon branches and spheroidization of the separated branches [17]. During solution treatment, the particles undergo changes in size and in shape. In the initial stages, the unmodified silicon particles undergo necking, acicular and separate into segments, which retain their original morphology. As a result of the separation, the average particle size decreases and the fragmented segments are eventually spheroidized. The spheroidization and the coarsening of eutectic Si can occur concurrently during the solution treatment.

Hurtalova et al [56] studied the changes in structural characteristics of hypoeutectic Al-Si cast alloy after age hardening. The results showed that the structure changes depend on age hardening. The heat treatment was observed to change the eutectic Si particles. The Si-platelets were spheroidized to rounded shape. The age hardening caused great changes of Fe-rich phases. Skeleton-like $Al_{15}(FeMn)_3Si_2$ phases were dissolved and fragmented. Spheroidization of eutectic Si, fragmentation of Al-Al_2Cu-Si and $Al_{15}(FeMn)_3Si_2$ phases were noticed to give better mechanical properties of recycled $AlSi_9Cu_3$ cast alloy.

Mohamed and Samuel [55] reported that the phases such as Al_2Cu and Fe- rich intermetallics, the dissolution rate is relatively slow. Even on prolonged solution heat treatment for some hours, these phases would not dissolve completely.

2.8 Development of Cast Aluminium Alloys for Cylinder Head Applications and Some Mechanical Properties

A recycled aluminium alloy for cylinder heads was developed and the chemical composition of the developed alloy is as shown in table 2.1 [14]. An alloy has been developed from scrap cylinder heads, which falls within the identified alloy chemical composition range. Secondary aluminium alloy has been obtained by melting different aluminium engine cylinder head scraps. Its fluidity and baseline mechanical properties have been investigated. The effect of minor elements such as Sr, Fe, Mn and different heat treatment parameters have also been investigated on the alloy and satisfactory mechanical properties and fluidity characteristics obtained. Common alloys used in cylinder heads were found to be of type 319.0, 356.0, 355.0, 354.0, A380.0. Chemical composition analysis of the scrap samples showed that most of them fall in the range of Japonese International Standard (JIS AC2B) alloy which is equivalent to 319.0 alloys [14]. This alloy has been recommended to be a potential candidate for production of cast aluminium alloys. Therefore, it is important to carry out further analysis on the effect of selected minor element on the microstructure and fatigue performance of this alloy.

Table 2.1: Chemical composition of alloy developed [14]

Alloy	Si	Cu	Mg	Fe	Mn	Cr	Zn	Ni	Ti	Pb	Sn
Base alloy	6.0	2.62	0.24	0.28	0.21	0.02	0.12	0.02	0.02	0.01	0.01

Ozbakir [17] studied development of aluminium alloys for diesel engine applications and concluded that, the trace additions of Cu, Zr, Mn and/or Cr did not seem to play an

important role in the SDAS of the permanent mould cast alloys. The combined addition of Cr, Zr, Mn and Cu gives the highest YS of the alloys.

Pavlovic [47] studied impact of casting parameters and chemical composition on the solidification behaviour of Al-Si-Cu hypoeutectic alloy. The service life of aluminium cast component is determined by the size, form and distribution of microstructure features throughout the casting, especially in those regions that are critically stressed. Grain size, SDAS, distribution of phases, the presence of secondary phases or intermetallic compounds, the morphology of silicon particles (size, shape and distribution) and finally, defects (porosity) play a key role in the behaviour of cast aluminium alloys.

Grosselle et al [24] studied correlation between microstructure and mechanical properties of Al-Si cast alloys and concluded that, the mechanical properties, i.e. the UTS and elongation to fracture of cast aluminium silicon alloys for cylinder heads depend on SDAS. Increasing the SDAS values decreases UTS and the elongation to fracture decrease. Grosselle et al [24] also reported mechanical properties are affected by microstructure. The best values of UTS and elongation to fracture are obtained for low SDAS values. Small and more compact eutectic Si particles, as well as a fine microstructure are attributed to high solidification rates in correspondence of casting. All of these desirable features of the cast structure are responsible for good mechanical properties associated with small SDAS [57].

2.9 Factors Controlling Fatigue Damage

2.9.1 Introduction

Fatigue is a phenomenon of damage accumulation at stress concentrations caused by fluctuating stresses and/or strains that may result in cracks or fracture after a sufficient number of fluctuations [58]. Fatigue fractures are caused by the simultaneous action of cyclic stress, tensile stress and plastic strain. If any one of these three is not present, fatigue cracking will not initiate and propagate. A fatigue crack is started by cyclic stress, whereas crack propagation is produced by tensile stress. In general, this phenomenon has attracted attention because progressively more and more is demanded from machine parts in term of speeds of operation and loads to be sustained [59]. The process of fatigue failure consists of three stages [59]

- Stage I - Initial fatigue damage leading to crack nucleation.
- Stage II - Progressive cyclic growth of a crack (crack propagation) until the remaining uncracked cross section of a part becomes too weak to sustain the loads imposed.
- Stage III - Final, sudden fracture of the remaining cross section.

The study of the fatigue performance of Al-Si alloys has had interest from several researchers for applications in critical components in automotive areas due to an array of attractive properties. In most of these applications, the components are subjected to high

load levels which are sometimes cyclic in nature; hence there is a need to develop of new Al-Si with better fatigue strength performance.

Research work has shown that in the fatigue of Al-Si alloys, there is agreement on the dominance of casting defects over all other established factors. These defects come in form of porosity (gas and shrinkage porosity), entrapped oxide films and sometimes-intermetallic inclusions. However, casting porosity is the main factor that influences negatively the fatigue properties of alloys [59, 60,61].

The scatter of fatigue properties in aluminium castings is due to the presence of casting flaws. Amount, size and locations of the flaws in components determine the fatigue performance of castings. Reducing flaw size increases fatigue life [11]. Other microstructural parameters such as the silicon particle size, distribution and shape have also been found to influence fatigue properties of cast aluminium alloys [62].

Fatigue crack initiation and growth behaviour is influenced by microstructural features, geometrical effects, loading conditions, surface and environmental effects. The total fatigue life of a component therefore incorporates the number of load cycles required to initiate a dominant crack and to propagate this crack until failure occurs.

2.9.2 Porosity Defects of Cast Al-Si Alloy

A bigger defect causes shorter fatigue lives while a surface defect of a given size can be more damaging than a large internal one. Moreover, presence of clusters of relatively small but numerous close pores accelerates the failure process not only by easier crack

propagation but also by collectively raising the stress concentration factor [23]. Porosity refers to voids or cavities that are formed within a casting during solidification and is a major cause of rejection in casting products. Porosity is caused by shrinkage resulting from the volume contraction associated with solidification as well as inadequate flow of molten metal and hydrogen gas evolution [35,64]. The size of a pore is, therefore, influenced not only by the hydrogen content in the melt, but also by cooling rate during solidification. A higher cooling rate reduces the pore size [35]. Porosity acts as the main crack initiation site leading to reduction in fatigue life especially as the size of the surface pore increases. The surface porosity is mainly responsible for decreasing the fatigue life of the specimens because it creates regions of high stress concentration [23].

Wang and Apelian [63] observed that fatigue lives generally vary inversely with the initiating pore size. Figures 2.6 and 2.7 are examples showing the distribution of total fatigue life with crack initiating pore size. Major [62] reported that as the pores size increased in A356-T61 Aluminum Alloy, the fatigue life also decreased.

Therefore, porosity is one of the major defects in aluminum castings alloys, which results in poor mechanical properties. Porosity can be reduced by subjecting castings to hot isostatic pressing. The hot isostatic pressing process removes the internal surface-connected porosities and improves the mechanical properties significantly [65].

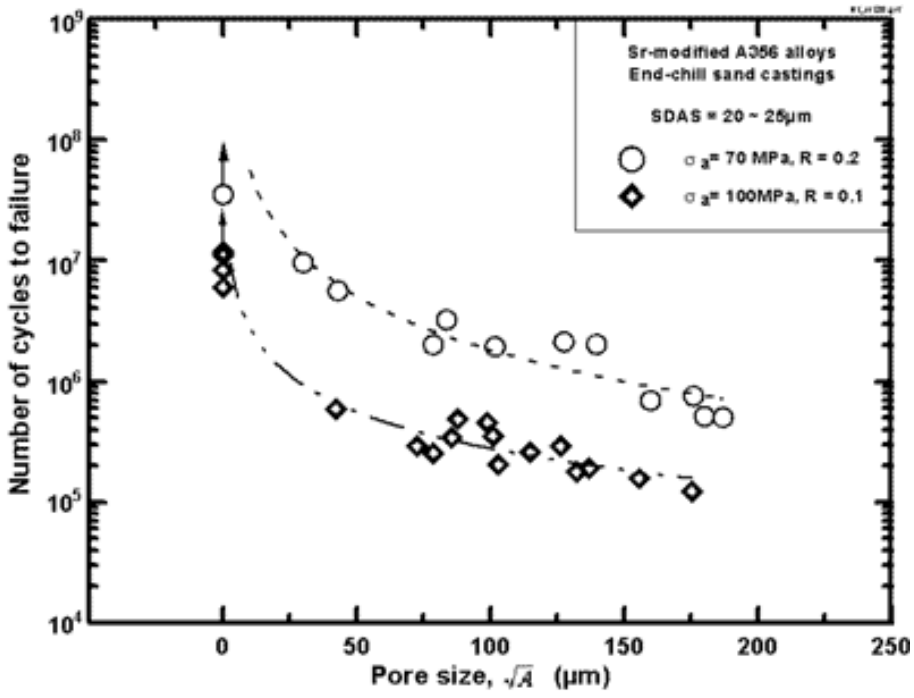

Figure 2.6: Distribution of Fatigue life of a Sr-modified A356-T6 alloy as a function of pore size; SDAS: 20-25μm [63]

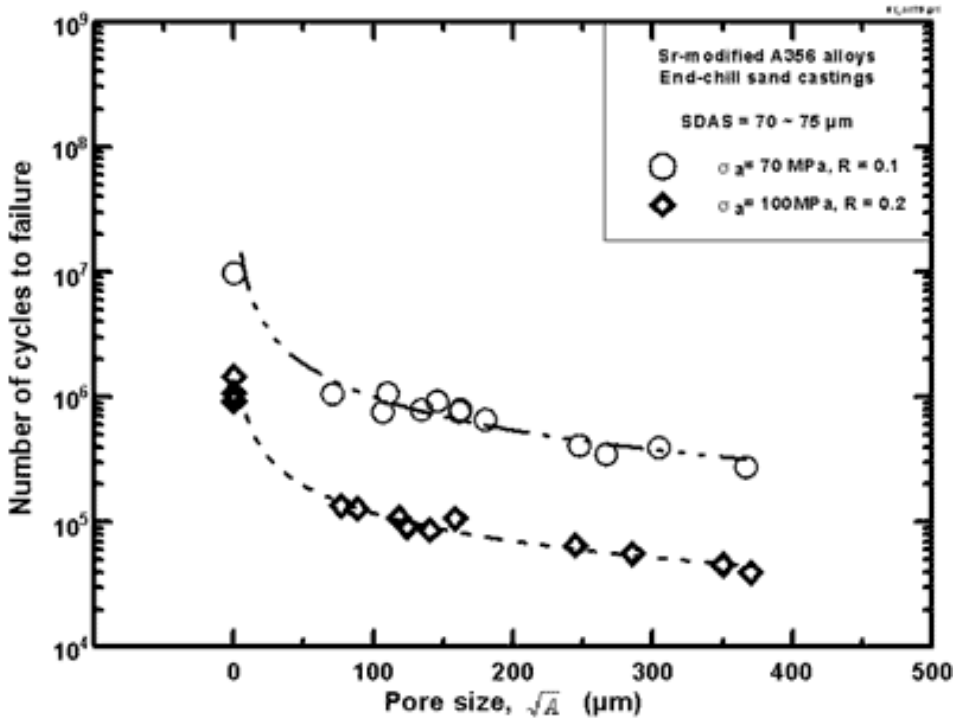

.

Figure 2.7: Distribution of Fatigue life of a Sr-modified A356-T6 alloy as a function of pore size; SDAS: 70-75µm [63]

2.9.3 Fatigue Crack Initiation

It is well known and documented that the fatigue process is very dependent on the surface state. Fatigue life of material is significantly affected by material surface finish and surface treatment; hence fatigue is a surface-sensitive process. In fact, fatigue cracks frequently nucleate on the surface of a metal. The nucleation as well as the entire fatigue process is partly controlled by casting defects. Therefore, crack nucleation is expected to occur in the spot where highest casting defects is experienced.

Fatigue initiated in aluminum casting alloys is almost always from the surface pores, inclusions or oxides films. In absence of such defects, crack initiation occurs at the fatigue-sensitive microstructural constituents. Fatigue crack may also initiate from cracking and decohesion of large silicon and Fe-rich intermetallic particles and crystallographic shearing from persistent slip bands in the aluminum matrix [11].

Mayer et al [65] reported that fatigue cracks initiate from surface or near surface pores. This is in agreement with Major [69] who observed that the fatigue crack nucleated from surface porosity in in A356-T61 Aluminum Alloy.

Zhu [43] observed that for tested samples, porosity was the source of the initiation of the crack that ultimately caused failure. In approximately 70% of the samples the fatigue crack initiated at a pore located at or near the specimen surface. It is reported [21] that large shrinkage pores promote the initiation of fatigue cracks, leading to premature failure of the samples with a high dispersion of data due to variability in the critical pore size.

The study [23] indicated that the fatigue crack initiation is influenced by size and localization of casting pores. Fatigue life increase if initiation places reduce in number. For a given number of initiations, an increase in pore size seems to reduce fatigue life.

McDowell et al [66] reported that when shrinkage porosity is controlled, the relevant micro-structural initiation sites are often the larger Si particles within eutectic regions. Mbuya et al [67] observed that cracks initiate from large particles and intermetallic

clusters as well as oxides. Mbuya et al [67] observed that the particles failed either by debonding at the interface with aluminium matrix or by cracking.

2.9.4 Fatigue Crack Propagation

In general, studies of fatigue propagation characteristics can be carried out in two ways: firstly, fracture mechanics behaviour studies in terms of fatigue crack growth rate as a function of the applied stress condition and secondly, investigation of micro mechanisms using scanning electron microscopy.

Crack growth is on the atomic level breakage and separation of the bonds linking the atoms and/or movement and gathering of dislocations (imperfections in the atomic structure). Therefore, new surfaces are created in the solid as the crack nucleates and continues to grow. This can be interpreted as an adaption of the material to an applied load of a critical level [68].

Fatigue crack growth behaviour usually refers to the plot of fatigue crack growth rate log (da/dN) against stress intensity range log ΔK. Based on the log (da/dN) against log ΔK plotted, the fatigue crack propagation process is divided into 3 regions as shown in figure 2.8. Region I indicates the region where the crack growth rate is assumed dormant or growing at an undetectable rate at low K values. In this region, crack propagation rates drop rapidly with decrease in ΔK towards the threshold stress intensity factor range ΔK_{th}.

Newman [69] indicated that fatigue crack growth threshold is a value of ΔK (crack-tip loading), below which no significant FCG occurs. Cracks are tolerated if ΔK is less than ΔK_{th}. However, FCG threshold is not constant. Many variables influence ΔKth including microstructure, environment, and load ratio. The value of crack growth threshold typically occurred below at 10^{-8} mm. For example Chen [70] has been found that the fatigue crack growth threshold value in cast aluminium(A356 alloy) in the region < 10^{-8} mm cycle to be approximately 5.2 MPa√m.

Region II, also called intermediate region of crack growth, the Paris-Erdogan equation describes well the growth of a crack with exponent m ranging typically between 2 and 5. In this region, the crack growth is controlled by continuous mechanisms, insensitive to the microstructure, average load, environment, and thickness of components.

$$\frac{da}{dN} = C(\Delta K)^{m} \qquad 2.1$$

Where C and m are constants and are dependent on the material, environment, frequency, temperature, and stress ratio. The fracture surface in this region is characterized by striations [71].

Crack behavior in Region III is related to unstable crack growth, as the maximum stress intensity factor (K_{max}) approaches the fracture toughness (K_c) of the material. In this region, crack growth is strongly sensitive to microstructure, load ratio (R) and mean stress. The fracture surface in upper Region III occurs almost entirely through a ductile static tearing of the large Al-Si eutectic Regions [71].

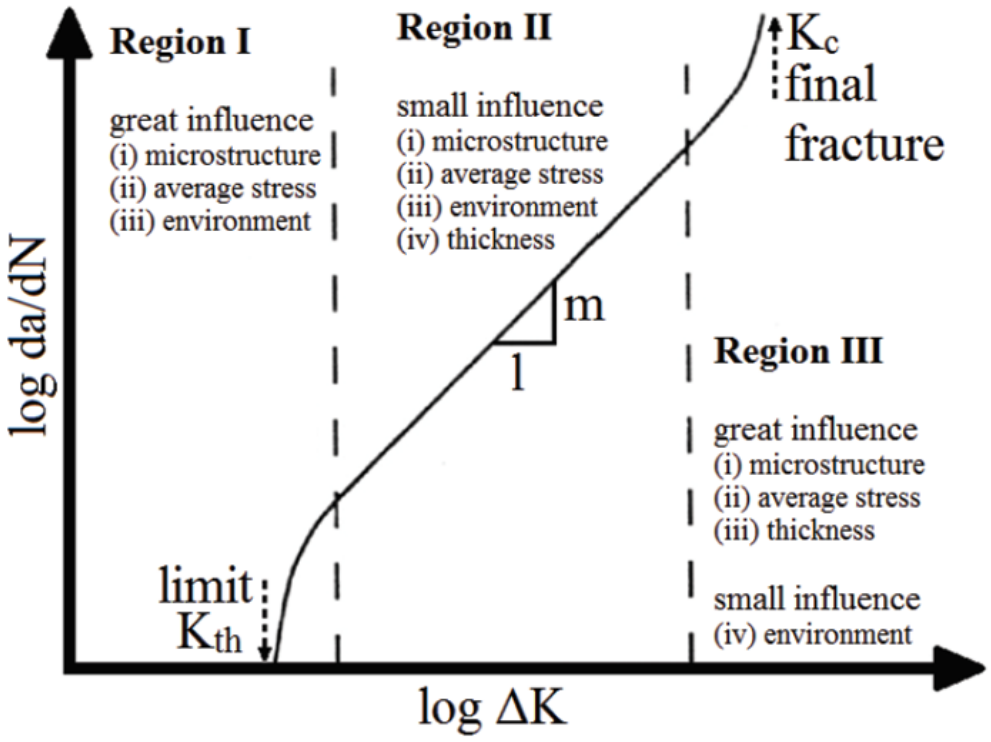

Figure 2.8: Typical long fatigue crack growth behavior [72]

2.9.5 Fatigue Life

Fatigue lives of material represent the time for a flaw to initiate and propagate to failure. The most frequent method used to evaluate the fatigue life of a material is to plot a Wöhler curve also called the S -N curve. An S-N curve is where, cyclic stress amplitude is plotted against the log number of cycles to fractures for a material [73,74]. This form of S-N curve shown in Figure 2.9, is significant in determining the stress below which the specimens does not fracture. This limiting stress is called the fatigue limit or endurance limit below which fatigue failure will never occur. Ferrous metals such as

steel have fatigue limit or endurance limits. But most non-ferrous metals do not have a fatigue limit. By conventionally, fatigue response of these materials is specified for a number of stress cycles, which is normally equal 10^7cycles [75].

Stanislava et al [23] noted the relation between stress amplitude and fatigue life show entirely high scatter. This was expected for cast Al-Si alloys because of the inhomogeneity of the cast material and casting defects. S-N curve is one of the important tools to visualize the time to failure of a specific smooth specimen material. Chen et al [76] studied the fatigue properties of aluminum 356 and 319 with and without hot isostatic pressing using S-N fatigue data. The fatigue life was significantly improved by hot isostatic pressing. For the A356 alloy at 125MPa, the fatigue life was improved from an average of 4.5×10^5 to 3.5×10^6. For the 319 alloy the fatigue life was improved from an average of 1.2×10^4 to 3.5×10^6.

Consequently, S-N fatigue curve is useful in determining fatigue strength and fatigue life performance of the material at different stress levels.

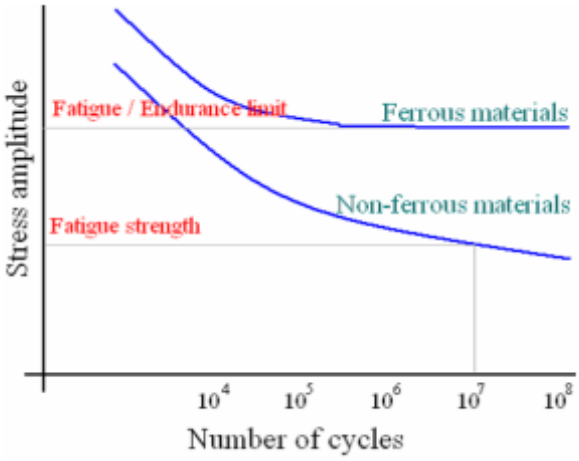

Figure 2.9: Typical S-N curves for ferrous and non-ferrous engineering metals

In summary: Al-Si alloys are the most used in industry because of their attractive properties such as good fluidity, welding suitability, good dimensional stability and low melting point. The demand of Al-Si alloys has increased in automotive applications due to their high properties; there is need to maximize mechanical properties of these alloys. One way has been to optimize alloying additions. Alloying elements have been observed to maximize the properties of the alloy. Some of elements may be added to form the intermetallic elements which results in the formation of casting defects such as porosity and oxide inclusions. However, the presence of Fe-intermetallic phases especially the brittle β-phase in the microstructure of cast Al-Si alloys causes reductions in mechanical properties. However, the deleterious effect of casting defects has also been recognized.

The mechanical properties of cast Al-Si alloys are directly affected by casting defects, but when reduced to low levels, other microstructural features become harmful to

mechanical performance. It is necessary to understand the effect of additives elements on the microstructural features and mechanical performance of cast Al–Si alloys.

Porosity is particularly detrimental to fatigue life when its size is larger than other microstructure features in the alloy due to its role in initiating fatigue cracks and facilitating their growth. Fatigue cracks usually develop from the largest pores located at or near the surface. The effects of surface pores on fatigue life increases as the pore size increases. When pore size is reduced cracks initiate from oxide films, eutectic Si and other intermetallic particles.

The best method used to evaluate the fatigue life of a material is S-N curve, which represents the stress amplitude against the time of cracks initiate up to failure in the alloys. The scatter in fatigue life is due to stress concentration and distribution of casting defects in the microstructure of the alloys for beginning fatigue cracks.

The aim of the study is to provide in-depth understanding of mechanical performance of a recycled Al-Si-Cu-Mg alloy for use in automotive engine cylinder heads in relation to microstructure.\

CHAPTER THREE

EXPERIMENTAL METHODOLOGY

3.1 Introduction

To achieve the objectives of this study, repeated experiments using rotating bending test machine under control load condition were carried out by varying applied load, calculating stress to failure at room temperature and plotting S-N results to analyze data. The alloy used in this study was obtained by melting different scrap cylinder heads from small vehicles. The specimens were prepared according to ASTM- E466 standard. Tensile specimens were also machined according to ASTM B557M standard.

3.2 Material and Method

The secondary aluminum alloy investigated was obtained by melting different aluminium engine cylinder head scraps in an oil fired graphite crucible furnace at Jomo Kenyatta University of Agriculture and Technology [14]. This research focused on testing fatigue performance and its relationships with the microstructure for the base alloy developed. The chemical composition of the base alloy is shown in Table 3.1. Some minor elements were added to examine their effect on the mechanical performance of this alloy.

Table 3.1: Chemical composition of base alloy

Alloy	Si	Cu	Mg	Fe	Mn	Cr	Zn	Ni	Ti	Pb	Sn

Base alloy	6.0	2.62	0.24	0.28	0.21	0.02	0.12	0.02	0.02	0.01	0.01

After adding master elements to the base alloy, composition of the new alloys is as shown in Table 3.2. Fatigue strength and its relationship with microstructure characterization were tested on four different alloy compositions developed as shown in table 3.2 in order to investigate the effect of adding different master alloys on the microstructure and fatigue life of recycled aluminium alloy for cylinder head applications.

Table 3.2: Alloy variants investigated

No	Alloys developed with total composition of each additive element in the alloy
1	BA
2	BA+0.02%Sr
3	BA+038%Fe
4	BA+0.9%Fe+0.45%Mn

3.3 Alloy Preparation

Melting of the cylinder head ingots to obtain cast bar was carried out in a 4 kg capacity SiC crucible using an electric muffle furnace at the University of Nairobi. (A photograph of electric muffle furnace used in this work is shown in Figure 3.1 (b)). Nitrogen gas was used to degas the molten metal by immersing a ceramic tube deep into the molten

metal to remove hydrogen in order to reduce porosity in the casting. Melting temperature was kept at 750^{o}C during pouring and a K-type thermocouple was employed to measure the temperature of the molten metal. Measured Fe, Sr and Mn master alloys were added to the molten base alloy at 750^{o}C to achieve target compositions. Strontium was added in the form of Al-10%Sr master alloy to achieve a 0.02wt% strontium concentration, whereas Fe and Mn were added in the form of Al-75%Fe and Al-75%Mn master alloys briquettes, to obtain a 0.9wt% Fe and 0.45wt% Mn concentrations respectively. After completely stirring to dissolution and homogenization of the alloy chemistry, the molten metal was skimmed to remove dross and surface oxides prior to pouring. The degassed molten metal was then poured into a permanent metal mould shown in Figure 3.2. The permanent metal mould was preheated to a temperature of 500^{o}C using an air circulated furnace shown in Figure 3.1 (a). A ceramic foam filter was placed in the mould for each casting to minimize turbulence during mould filling and for trapping of inclusions. After solidification the two half's of the mould were separated and the cast bar removed shown in Figure 3.3.

The sample bars were then sectioned from different positions in order to obtain different specimens for tensile testing, fatigue testing and specimens for microstructure analysis. The test samples were evaluated both in the as-cast condition and in a T6 heat treated condition.

Figure 3.1: a) Air circulated furnace and b) Electric muffle furnace

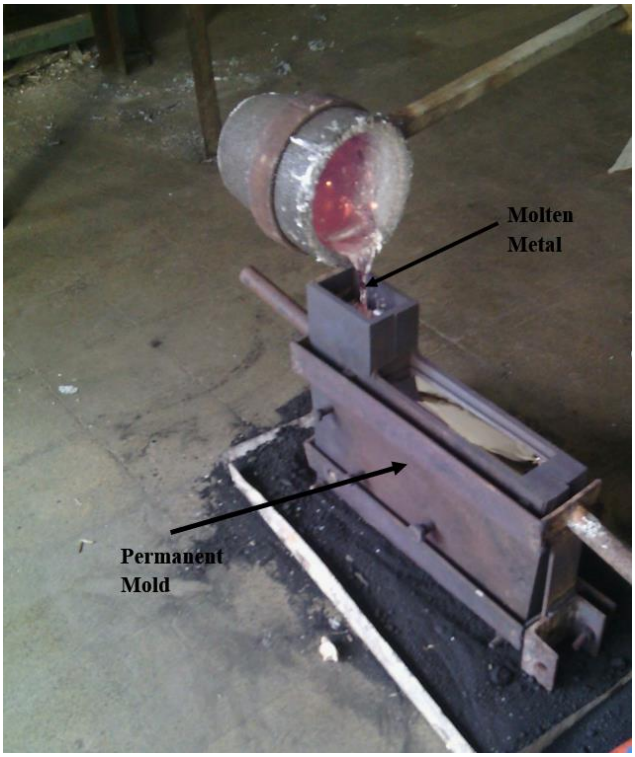

Figure 3.2: Permanent cast iron

Figure 3.3: Cast Bar

3.4 Heat Treatment

The cast parts were heat treated in an air circulated electric resistance furnace with a temperature controller for both solution and aging heat treatments shown in Figure 3.4. The solution heat treatments were carried out for 6 hours at 495^0C. The solution heat-treated samples were then quenched in warm water (65^0C) followed by naturally aging for 24 hours and artificial aging for 10 hours at 170^0C.

Figure 3.4: A photograph of the air circulated electric resistance furnace used for heat treatment.

3.5 Microstructure Examination

Microstructure analysis was done on samples cut and prepared from the casting using Optika-optical microscope B-350 MET at University of Nairobi. Each specimen was ground by successively rubbing on different grades of 240, 320, 400 and 600 SiC paper under flowing water. The specimen was then washed with running water to remove debris associated with the grade of paper used. It was thereafter ground on the next finer paper such that the scratches produced are at right angles to those formed by the previous paper. This was achieved by rotating the specimen 90^0C between grinding steps. After the last paper, the specimen was washed well in water and then methanol and dried. The ground specimens were successively polished on a rotating wheel using 6µm, 1/4 µm and 1µm. They were then washed with water and methanol and hot-air dried. The polished samples were observed in an optical microscope Figure 3.5, after which their images were taken for microstructural analysis. A more detailed intermetallic phases observation in the alloy variants was done by using scanning electron microscopy (SEM) connected to Energy-Dispersive X-ray Spectrometry (EDS).

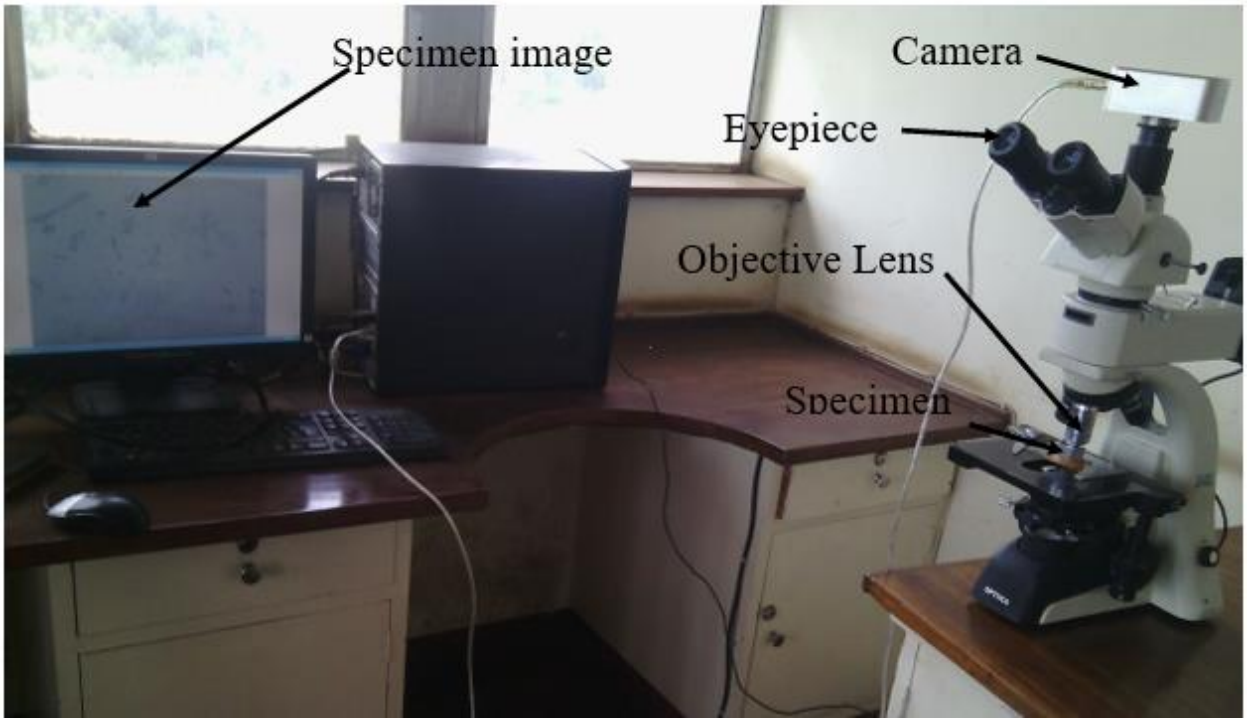

Figure 3.5: Optical microscope used in this study

3.6 Tensile Testing

The tensile test specimens were prepared according to the ASTM B557M standard with a gauge length of 25.4 mm and gauge diameter of 6.35mm as shown in Figure 3.6. The specimens were tested using the Hounsfield Tensometer testing machine located at University of Nairobi. Three specimens were tested for each alloy to obtain three data points from which an average value was taken. After fracturing the tensile test specimens, the two pieces were reassembled and the new gauge length obtained and % elongation to fracture determined using equation 3.1.

$$\%el = \frac{Lf - Li}{Li}$$

3.1

Where Lf: Final gauge length and Li: Initial gauge length.

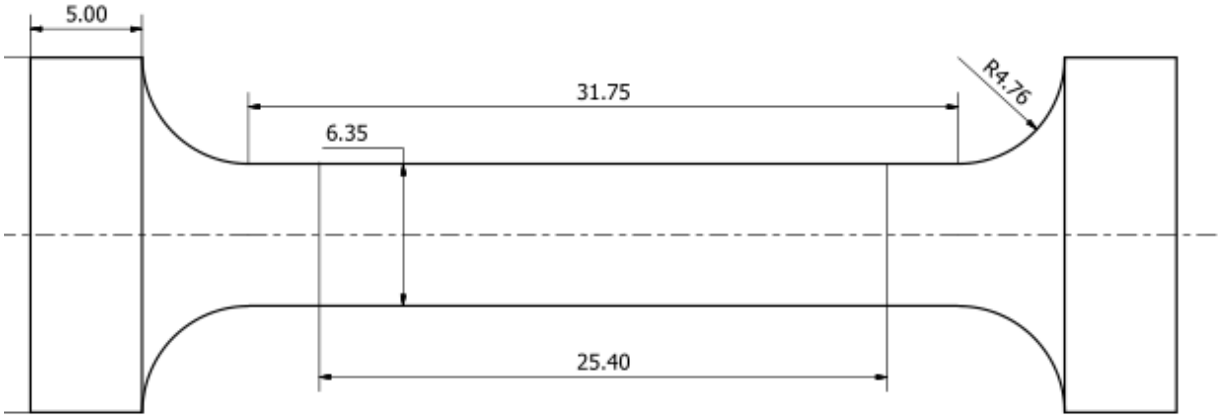

Figure 3.6: Dimensions of tensile specimens

3.7 Fatigue Testing

Characterization of fatigue behavior in terms of nominal stress (S - N curve characterization) was performed using a rotating bending fatigue test machine at University of Nairobi. A photograph of rotating bending fatigue test machine used in this work is shown in figure 3.8. Specimens for fatigue testing were prepared after T6 heat treatment. Specimens for fatigue tests were machined from each type of alloy to dimensions shown in figure 3.7 (a). Figure 3.7 (b) shows machined fatigue test

specimens. The sizes of the specimen were defined according to the ASTM-E466 Standard. Fatigue life curves for different sets of specimens were obtained using smooth 4-mm-diameter fatigue specimens subjected to rotating bending loading at 50Hz frequency, fully reversed and under a stress ratio of R = -1. Six specimens for each alloy were tested, 3 of them under high load and the rest under low load. The specimen was subjected to load at its free end perpendicular to its axis while rotating. This caused a bending moment which can be calculated by using the following equations:

$$\sigma b = \frac{M.r}{I} \quad 3.2$$

$$\sigma b = \frac{P.L.r}{\frac{\pi \times d^4}{64}} \quad 3.3$$

$$\sigma b = \frac{P.L}{\frac{\pi.d^3}{32}} \quad 3.4$$

Where:

σb : Bending stress

M: Bending moment

r: Neck diameter of specimen

L: Distance from the load to the neck of specimen

I: Moment of Inertia ($\frac{\pi.d^4}{64}$)

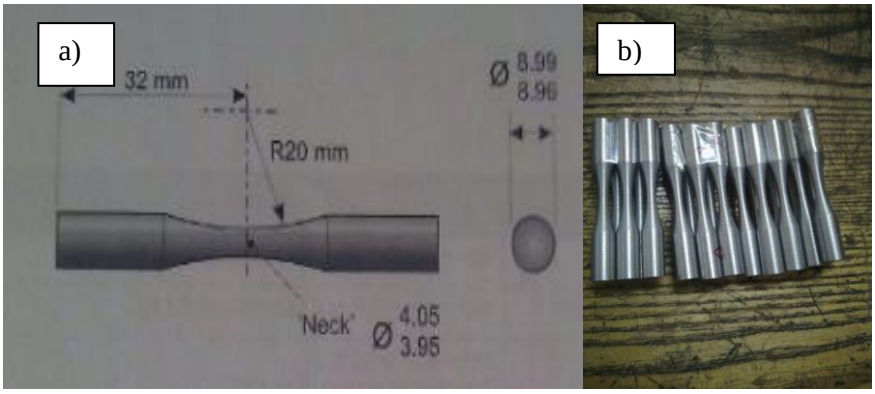

Figure 3.7: a) Standard fatigue specimen dimensions b) Fatigue specimens machined from cast bar

Figure 3.8: Rotating bending fatigue test machine

CHAPTER FOUR

RESULTS AND DISCUSSION

4.1 Introduction

Examination of fatigue behavior of the cast Al-Si alloys for cylinder head applications was carried out using S-N tests. It was found that minor changes in chemical composition affected the fatigue performance as well as tensile strength of the alloys investigated. Whereas some elements enhance the mechanical properties of the alloys, others marred the mechanical properties. This chapter discusses the results.

4.2 Microstructure

4.2.1 Optical/SEM Observations and EDS Analysis of as Cast Microstructure Alloys

Figure 4.1(a), shows an optical micrograph of the microstructure of base alloy for as-cast sample obtained without additional alloying. The microstructure characterization of the base alloy consisted mainly of the Al-matrix and coarse acicular Si particles. The SEM micrograph (Figure 4.1 (b)) revealed the presence of intermetallic phases in the base alloy. The intermetallic phases have been confirmed by Energy Dispersive X- ray Spectroscopy (EDS) analysis and are mainly Al_2Cu and AlCuNi. These kinds of intermetallic phases contribute to deterioration of mechanical properties of the alloy.

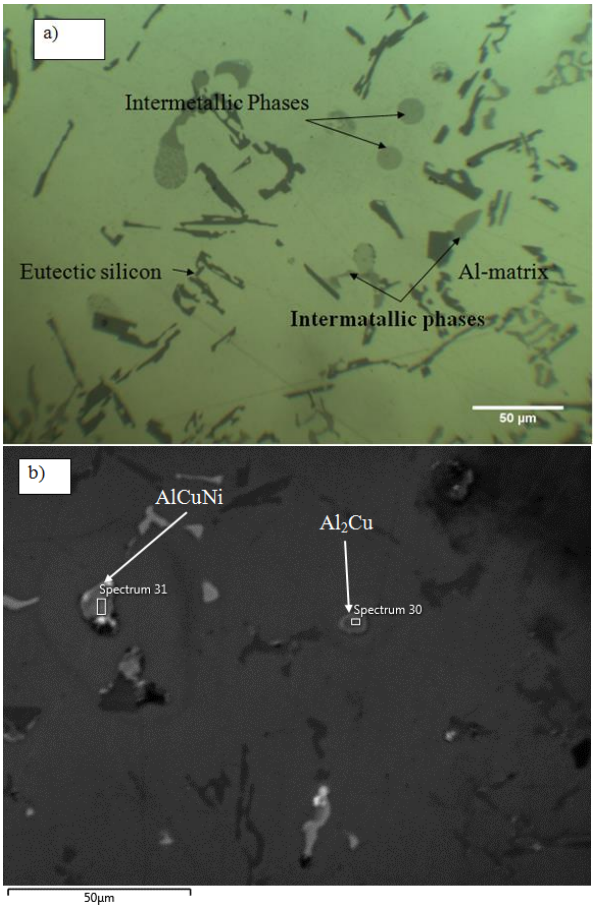

Figure 4.1: As cast microstructure of the base alloy. (a) Optical image; (b) SEM image

Figure 4.2 (a) presents the microstructure of the base alloy modified with 0.02 wt. % Sr. The micrograph shows that some coarse acicular Si particles were modified to a fine fibrous form; others partially modified. Intermetallic phases were also found in this alloy as shown in Figure 4.2 (b). The α-AlFeMnSi were identified in this alloy as it was confirmed by EDS analysis. These phases are fine and compact due to the refinement effect of Sr in the microstructure.

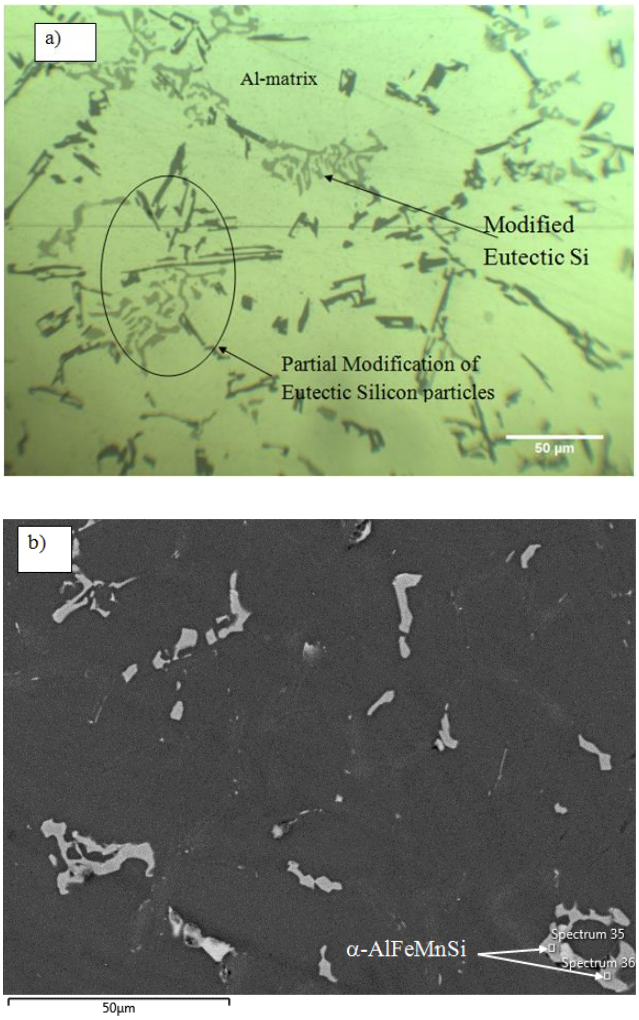

Figure 4.2: As cast microstructure of the BA+0.02%Sr. (a) Optical image; (b) SEM image

Figure 4.3 (a) shows the microstructure of base alloy with 0.38% Fe. Addition of 0.38%Fe in base alloy results in the formation of eutectic silicon particles in the aluminium matrix. Large eutectic silicon particles appeared in this alloy. These particles are usually origin of a material to failure. The microstructure does not show much difference

with that of the base alloy in Figure 4. 1. However, Al_2Cu and Fe rich phases were found in this alloy as shown in Figure 4. 3 (b).

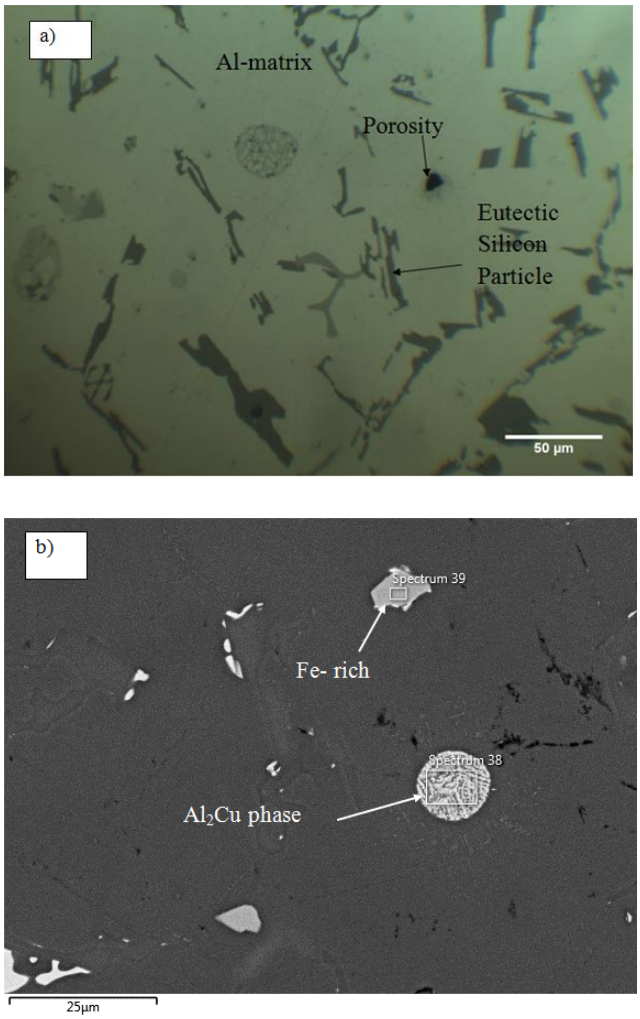

Figure 4.3: As cast microstructure of the BA+0.38%Fe. (a) Optical image; (b) SEM image

Figure 4.4 (a) reveals the microstructure of base alloy with 0.9%Fe and 0.45%Mn. The optical micrographs identified acicular eutectic silicon particles and the Al matrix. Beside silicon particles and Al-matrix, SEM/EDS analysis shows the intermetallic

phases, namely Al_2Cu and α-AlFeMnSi with Chinese script morphology shown in Figure 4.4 (b). An iron addition lead to the formation of β intermetallic phase and Mn addition eliminates the formation of β phase. Fang et al [36] reported that Mn addition decreased the detrimental effects of the Fe-rich phases by replacing it with the less detrimental Chinese script α -Fe phase, resulting in the improvement of mechanical properties.

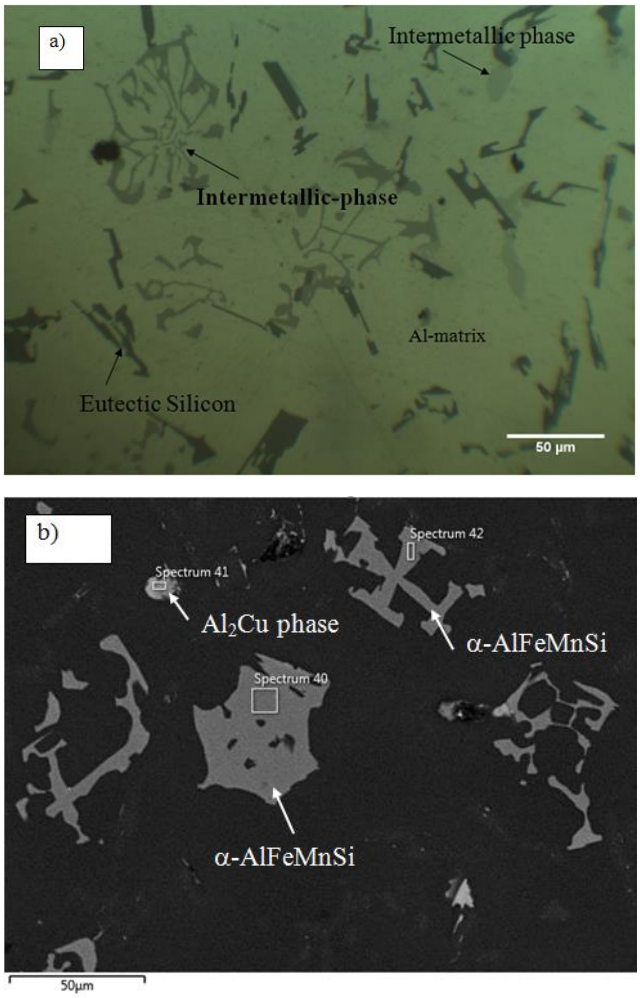

Figure 4.4: As cast microstructure of the BA+0.9%Fe+0.45%Mn. (a) Optical image; (b) SEM image

4.2.2 Heat Treated Microstructure

The microstructures after T6 heat treatment of alloys is shown in Figure 4.5, 4.6, 4.7 and 4.8. The metallographic characterization of the samples machined from cast alloys of cylinder heads showed that the microstructure primarily composed of primary -Al phase surrounded by the eutectic Si particles, porosity and intermetallic phases.

Figure 4.5 (a) illustrates the microstructure of base alloy after T6 heat treatment. It was observed that the base alloy has primary Al matrix with evenly distributed intermetallic phases, fragmentation of eutectic Si particles and eutectic Si particles. Si particles also appeared as coarser acicular shape due to the size and shape of particles. Eutectic Si was observed as long particles. The spheroidization and coarsening of particles is dependent on their initial sizes and shapes. The small particles are fast spheroidized and vice versa. Figure 4.5 (b) shows intermetallic phases observed using SEM/EDS analysis. The Iron intermetallic phase, eutectic Si particles and Al-matrix Phases were identified. The Al_2Cu was dissolved completely after T6 heat treatment.

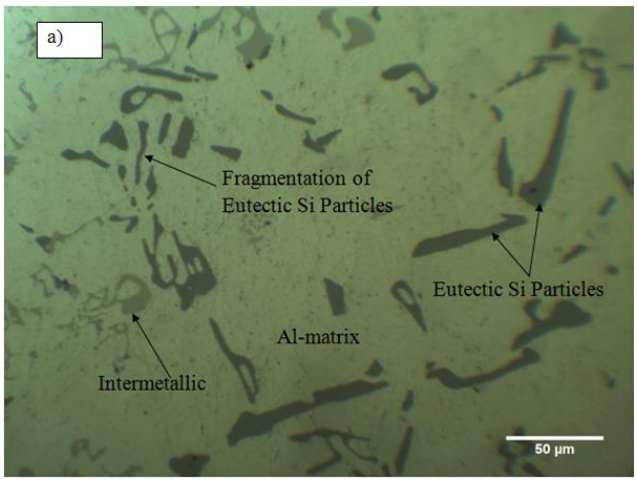

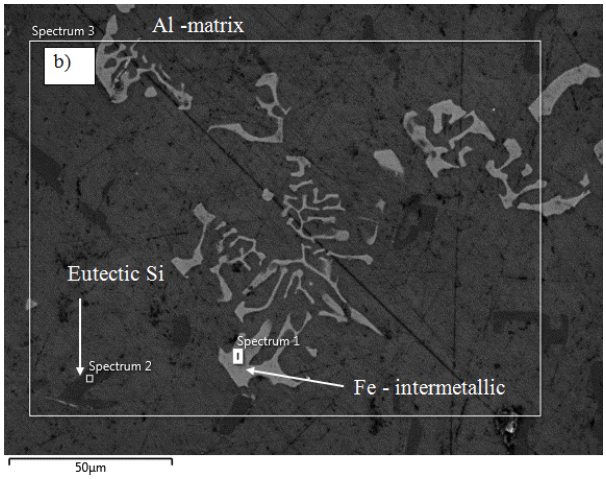

Figure 4 5: Heat treated microstructure of the base alloy. (a) Optical image; (b) SEM image

Figure 4.6 (a) shows the microstructure of base alloy modified by 0.02% Sr after T6 heat treatment. The micrograph of this alloy indicates the aluminium matrix surrounded by spheroidised eutectic Si particles and intermetallic phases. The micrograph revealed that the size of eutectic silicon particles is small and more compacted which led to a fine microstructure. The modifications of intermetallics were also fragmented shown in Figure 4.6 (b). It has been reported that the addition of strontium changed the eutectic Si morphology from acicular fibrous to round thereby refining the morphology of intermetallic phases [77].

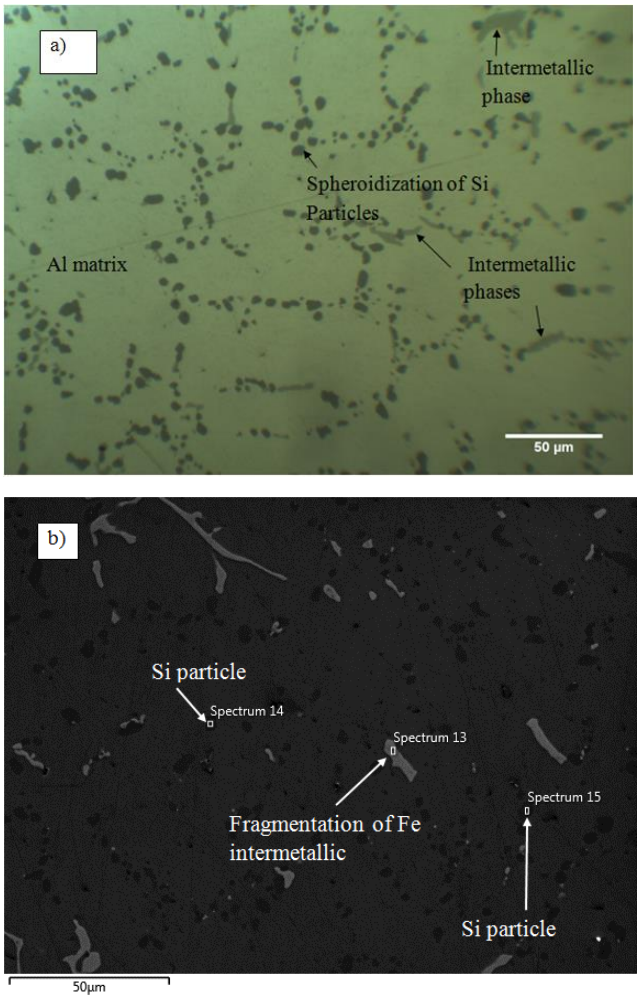

Figure 4.6: Heat treated microstructure of the base alloy with 0.02%Sr. (a) Optical image; (b) SEM image

The microstructure of base alloy with 0.38% is shown in Figure 4.7. The optical micrograph of this alloy shows primary Al- matrix surrounded by fragmented of silicon particles and intermetallic phases. Spheroidization of the eutectic silicon particles is not observed in this alloy after T6 heat treatment. The increase of iron to 0.38 wt. %Fe is

seen to significantly increase the size of the eutectic silicon particles. SEM/EDS indicate AlFeMnSiCu and Fe intermetallic phases in this alloy.

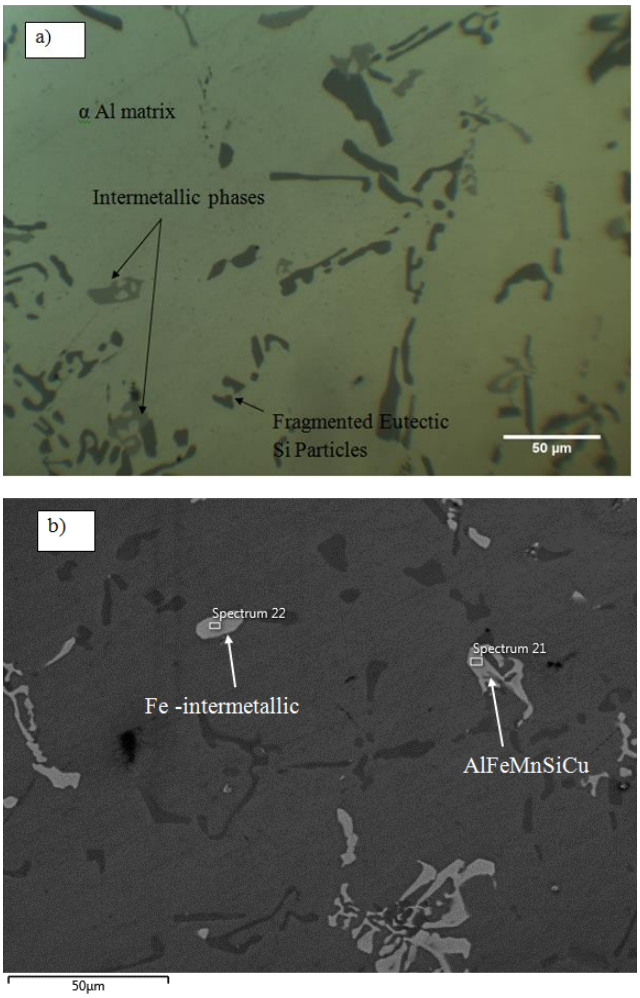

Figure 4.7: Heat treated microstructure of the base alloy with 0.38%Fe. (a) Optical image; (b) SEM image

Figure 4.8 illustrates the microstructure of base alloy with 0.9%Fe and 0.45%Sr after T6 heat treatment. Two phases namely, Iron intermetallic and α-AlFeMnSi phases were identified by using SEM/EDS. Fragmentation of eutectic silicon particles were found in

this alloy after T6 heat treatment. Dissolution of Al_2Cu phase in the Al-matrix was also obsessed.

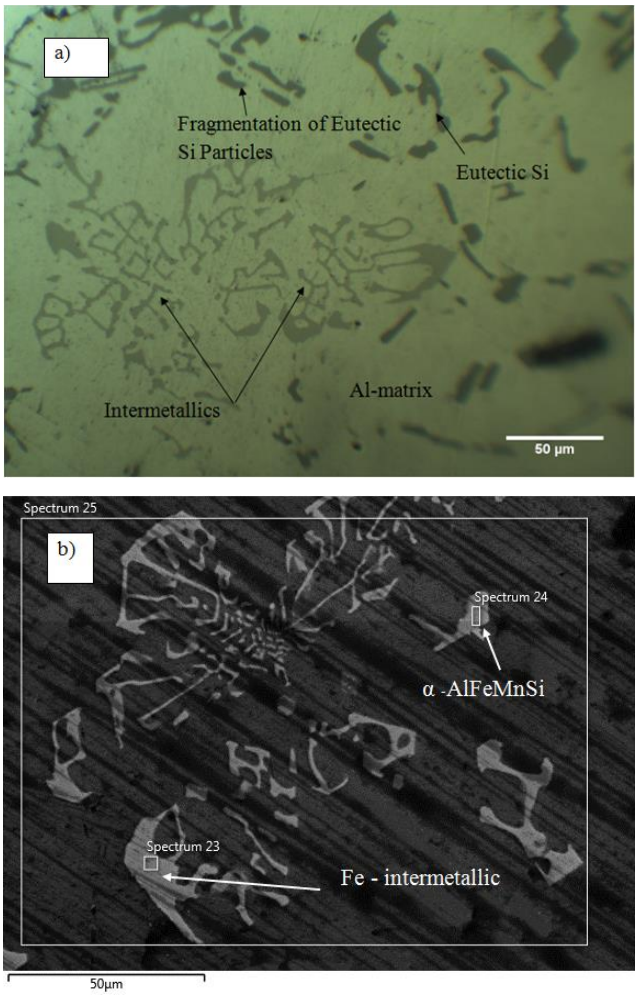

Figure 4.8: Heat treated microstructure of the base alloy with 0.9%Fe+0.45%Mn. (a) Optical image; (b) SEM image

4.3 Tensile Strength Tests

Figure 4.9 shows the average ultimate tensile strength (UTS) values for BA, BA+0.02%Sr, BA+0.38%Fe and BA+0.9%Fe+0.45Mn alloys in as cast material and

after T6 heat treatment. The value of UTS for each of the three specimens tested per alloy is shown in Appendix (Table A 1) and then average was taken.

It was observed that the average values of UTS were 163.12 MPa, 178.06 MPa, 149.92 MPa and 161.05 MPa respectively in as cast condition. While the average values of UTS were 220.85 MPa 250 MPa, 216.5 MPa and 235.23 MPa in T6 condition.

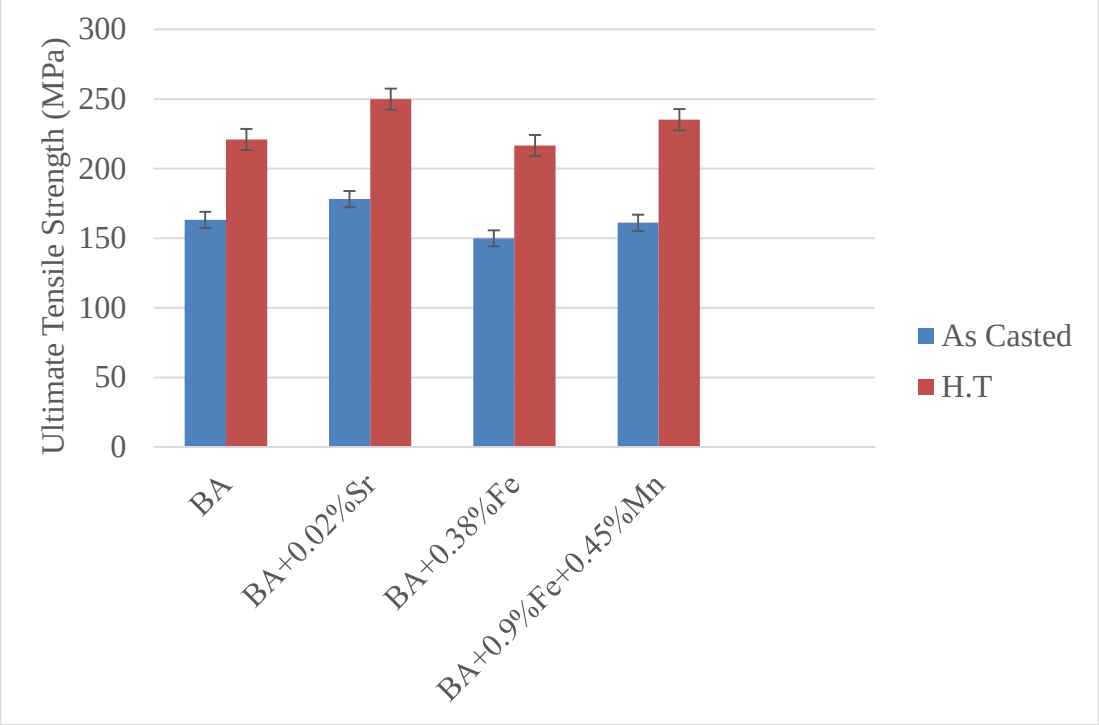

Figure 4. 9: Ultimate tensile strength

With addition of Sr level of 0.02% the average value of UTS increased by 9.15% in as cast condition. This increase was due to the power of strontium addition in modification of eutectic silicon particles. The addition of Fe level of 0.38% in the base alloy was

observed to decrease UTS by 8.1% in as cast state. Increasing iron content in the alloy led to the formation of intermetallic phases precipitated Al_2Cu and Fe rich phases, which contributed to the degradation of the mechanical properties due to their poor bonding strength with the matrix [7] and acted as stress raisers. It was observed that combining 0.9%Fe with 0.45%Mn in the base alloy decreased UTS by 1.3% in as cast alloy. The addition of Fe and Mn to the base alloy led to better UTS than the addition of Fe to the base alloy. This is because of the neutralizing effect of Manganese on Fe. The iron rich intermetallic phase was transformed to α-AlFeMnSi with Chinese script morphology that has probably less harmful effects on the mechanical properties.

After T6 heat treatment to the alloys (BA, BA+0.02%Sr, BA+0.38%Fe and BA+0.9%Fe+0.45%Mn) it was observed that the average values of UTS were 220.85 MPa, 250 MPa, 216.5 MPa and 235.23 MPa respectively. The addition of 0.02%Sr was found to increase the UTS by 13.2% while the addition of 0.38% Fe decreased UTS by 2%. However, addition of 0.9% Fe and 0.45%Mn slightly increased the UTS by 6.4%. The addition of strontium increased UTS by 13.2%, and this was due to the spheroidization of the eutectic Si particles, dissolution and fragmentation of intermetallic phases. Similar results obtained by Peng et al [78] reported that the UTS is influenced by the spheroidation of eutectic silicon particles and dissolution of intermetallic phases.

After T6 heat treatment, the average UTS of the alloys is indicated to increase by 35.4%, 40.4%, 44.4% and 46% respectively as compare to as cast alloys. Heat treatment was observed to improve the UTS for all alloys investigated, this was due to the age-

hardening that enhances the change in microstructure by spheroidization and coarsening of eutectic silicon, shortening and thinning of intermetallic phases. The dissolution of precipitates and the precipitation of finer hardening phase resulted in the increase in the tensile strength in the alloy [79].

4.4 Percentage Elongation

Figure 4.10 illustrates the average percentage elongation of the alloys in as-cast and after T6 heat treatment condition. The values of percentage elongation for each the three specimens tested per alloy is shown in Appendix (Table A 2) and then average value was obtained.

It was observed that the average percentage elongation in as cast condition of BA, BA with 0.02%Sr, BA with 0.38%Fe and BA with 0.9%Fe+0.45% Mn were found to be 1.4%, 1.67%, 1.08%, 1.26% respectively. For the base alloy modified by 0.02% Sr, the percentage elongation of the alloy increased by 19.28% while addition of 0.38%Fe decreased the percentage elongation of the alloy by 22.8%. With 0.9%Fe and 0.45%Mn addition, the percentage elongation of the alloy decreased by 10%.

Fine eutectic silicon particles and proper distribution of intermetallic phases in the casting resulted in improving the ductility [29]. The addition of strontium increased ductility in Sr-modified alloy due to modification of eutectic silicon particles. Acircular structure of the unmodified eutectic silicon particles and brittle intermetallic phases

resulted in inferior mechanical properties such as percentage elongation and strength. This is because they easily break due to their brittleness.

After T6 heat treatment, the average percentage elongation values of BA, BA with 0.02%Sr, BA with 0.38%Fe and BA with 0.9%Fe+0.45% Mn were 1.02%, 1.05%, 0.91% and 1% respectively. It was noticed that changes in alloy chemical composition caused slight effect on the percentage elongation of the alloys. During heat treatment, the hardness of matrix can cause reduction in % elongation of alloys. In the current study, the base alloy with 0.38%Fe was observed to have the smallest value of % elongation after T6 heat treatment. This was attributed to the large eutectic silicon particles observed in this alloy after heat treatment, which could significantly cause the failure of a material in the form of brittle fracture, thereby resulting in low ductility. Casting porosity may also have negative effect on tensile strength and ductility of alloys.

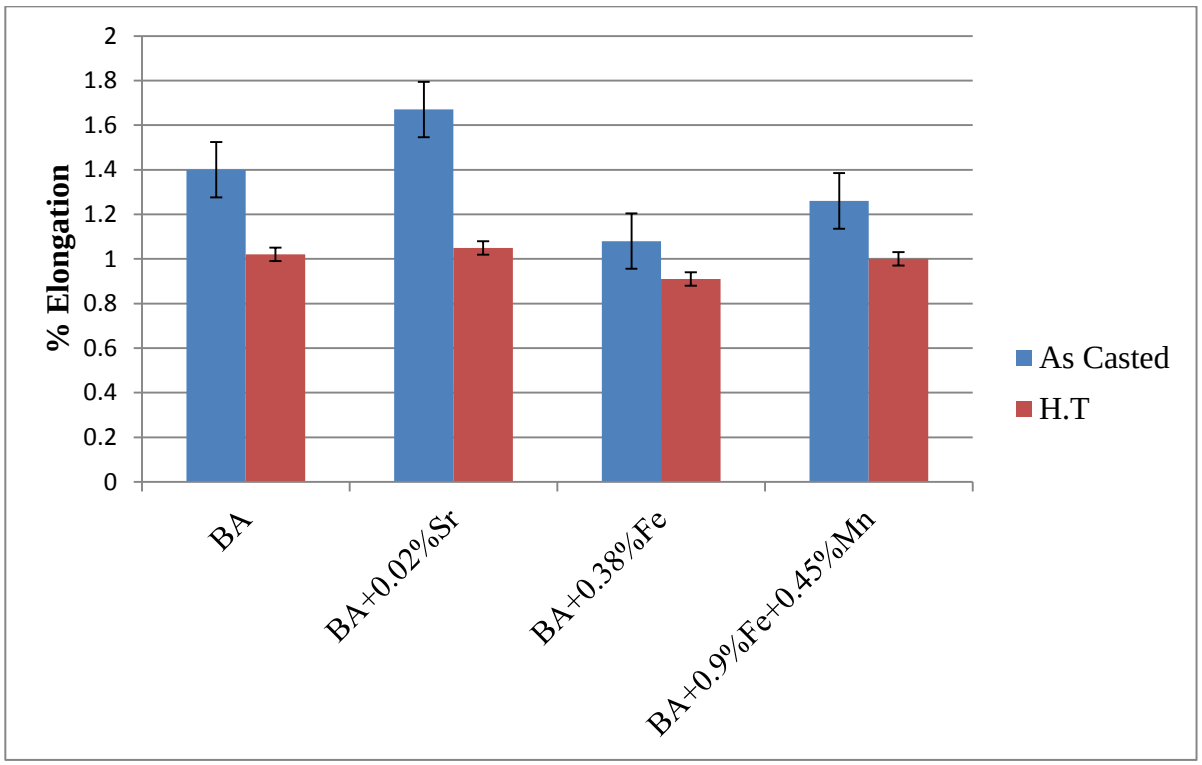

Figure 4.10: Percentage elongation of alloys tested

4.5 S-N Fatigue Data and Life Distribution

S-N fatigue data obtained from experiment are shown in table 4.1, Figure 4.11 and Figure 4.12. The figures illustrate the fatigue strength against the total fatigue life cycles of all the alloys investigated in this study. It is noted that the fatigue data obtained exhibit significant scatter which is a typical fatigue life distribution. Fatigue life behavior of material is significantly influenced by distribution of casting defects and intermetallic particles [11]. Different output of alloys can still be inferred from this data.

A comparison of the alloys examined shows that the BA+0.02%Sr has the highest fatigue life performance than those of BA and BA+0.38%Fe, BA+0.9%Fe+0.45%Mn in as cast condition and after T6 heat treatment. This value was attributed to the capacity of strontium addition in modification of eutectic silicon particles. Strontium addition refines grain size and modifies eutectic silicon morphology that results in improvement of fatigue performance of alloys due to minimizing casting defects [30]. It is agreeable that in unmodified Si particles the cracking is through Si particles. When the size of the eutectic Si particles reduces due to modification, the crack has to propagate through the more ductile Al matrix, which requires more time to failure. Therefore, the fatigue performance is highest in the Sr-modified alloy.

The BA+0.9%Fe+0.45%Mn was also observed to have good fatigue performance as compared to the base alloy with iron, this is because the addition of manganese to the alloy neutralized the iron effect. This improvement was attributed to the presence of iron rich intermetallic phase that was transformed to α-AlFeMnSi with Chinese script morphology which were precipitated during solidification. This in agreement with authors [36] who reported that Mn addition to the alloy decreased the detrimental effects of the Fe-rich phases by changing it to less detrimental Chinese script α-Fe phase, this leads to increase fatigue performance.

The BA+0.38% Fe exhibited the lowest fatigue life as compared to the other alloys. This was due to the presence of iron rich intermetallic phases in the alloy,that was probably initiated crack due to their stress raisers. They may also increase the porosity in the casting

due to the blocking the channels that feed solidification shrinkage and could influence the matrix stiffness.

The Figure 4. 11 and Figure 4.12 indicate that the T6 heat treatment does not improve the fatigue performance of base alloy and base alloy modified by strontium. This deterioration was related to the casting porosity that cannot be eliminated by applied heat treatment. The presence of pores in the microstructure of alloy reduces the number of loading cycles required to initiate a crack as well as to propagate a crack until the specimen failed. The casting porosity and intermetallic phases were most preferable to initiate a crack in the specimen during testing. For instance, in the base alloy the crack initiation site is as shown in Figure 4.13. Intermetallic particles can be seen in this region. Using EDS analysis, the initiating particle was identified to be the Al_2Cu phase. In contrast, T6 heat treatment was slightly improved the base alloy with iron and base alloy with iron + manganese. The improvement resulted in the blockage of the crack propagation by microstructure features impediment produced by the applied heat treatment , it was also due probably to their capacity of retardation of crack during propagation [54]. It is well known that in spheroidization and fragmentation of Silicon particles, the crack has propagate through in more ductile aluminium matrix that could probably delay the material to failure.

	Number of cycles to failure

Table 4.1: Number of cycles to failure of alloys tested

Alloys	Limit Stress(MPa)	Specimen No	As cast condition	Mean	H.T condition	Mean
BA	80	1	259,544	110,514	70,818	66,655
		2	33,805		67,820	
		3	38,193		61,328	
	130	1	66,711	61,806	25,301	18,911
		2	58,576		7,883	
		3	60,132		23,548	
BA+0.02 %Sr	80	1	810,755	610,399	93,598	160,745
		2	484,303		83,009	
		3	536,140		305,629	
	130	1	66,711	61,806	25,301	18,911
		2	58,576		7,883	
		3	60,132		23,548	
BA+0.38 %Fe	80	1	75,590	42,320	96,867	73,270
		2	18,221		45,696	
		3	33,148		77,248	
	130	1	24,362	15,465	8,907	6,999
		2	1,887		4,641	
		3	20,147		7,450	
BA+0.9% Fe+0.45 %Mn	80	1	86,929	97,314	200,598	145,060
		2	98,555		99,564	
		3	106,457		135,018	
	130	1	57,581	47,086	65,678	43,054
		2	42,167		51,789	
		3	41,511		11,696	

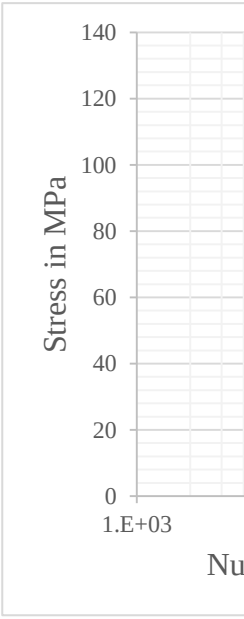

Figure 4.11: As cast

ed and Heat treated S-N results of stress versus number of cycles to failure

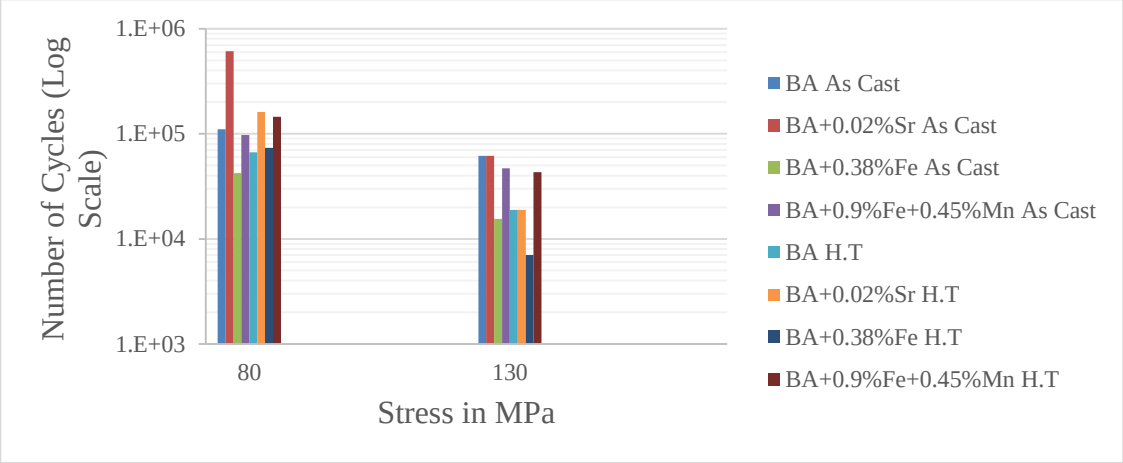

Figure 4.12: Bar Graph shown as casted and Heat treated S-N results of stress versus number of cycles to failure

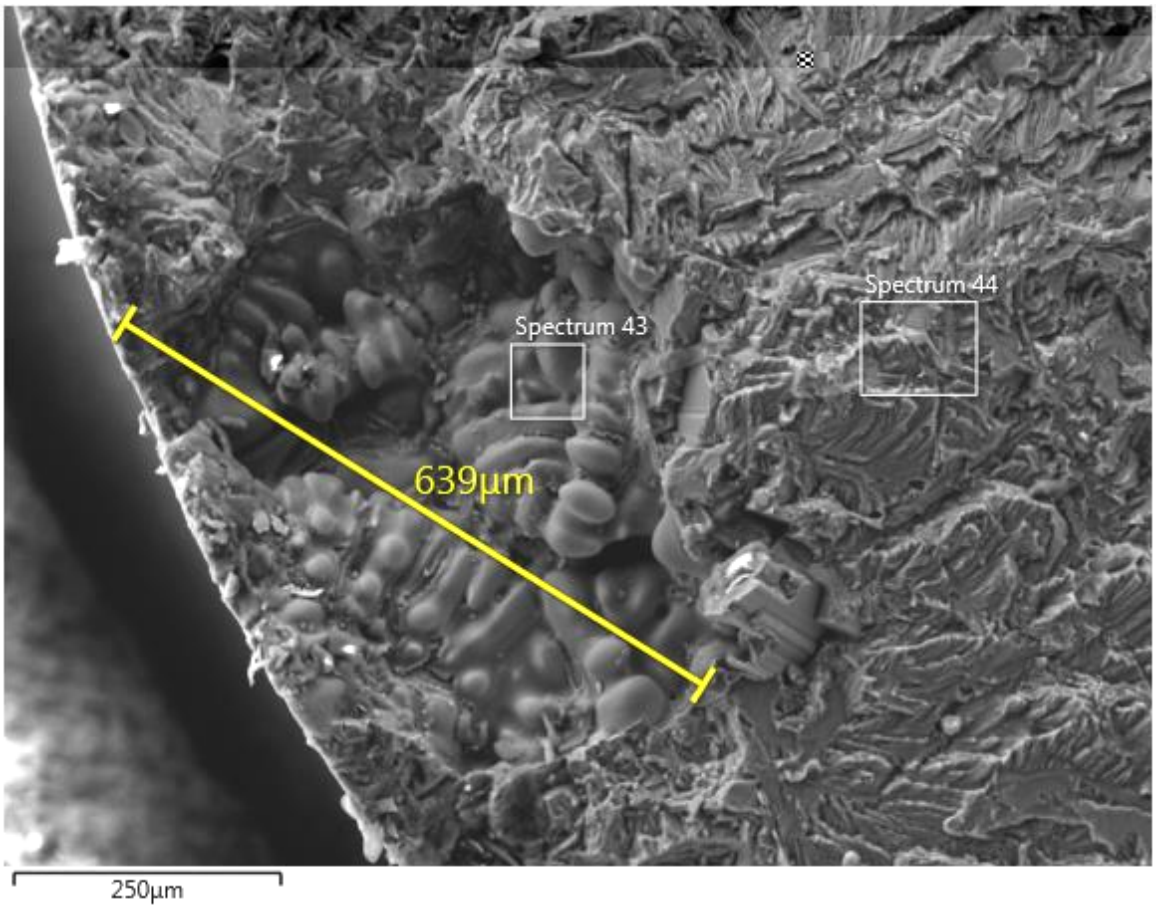

Figure 4.13: SEM image showing crack initiation at Al_2Cu phase

CHAPTER FIVE

CONCLUSION AND RECOMMENDATIONS

5.1 Concluding Remarks

This research was focused on the effect of minor elements (Sr, Fe and Mn) on the microstructure, fatigue performance and tensile properties of cast Al-Si alloy for cylinder head. Referring to the results obtained and their analysis, the following conclusions are drawn:

i. Addition of Sr, Fe and Mn on the microstructure of a secondary Al-Si-Cu-Mg alloy resulted in alloying elements have significant influence on the microstructural features of the alloy. The microstructure features of base alloy consisted mainly of a structure with primary Al-matrix, coarse acicular Si particles and intermetallic phases such as Al_2Cu and Al-Cu-Ni. When 0.02%Sr was added to the base alloy, coarse acicular Si particles were modified to a fine fibrous form. With addition of 0.38%Fe, results in the formation of large eutectic silicon particles and Fe rich intermetallic phase. Moreover, when 0.45%Mn was added in combination with 0.9%Fe, the Al_2Cu, and α-AlFeMnSi with Chinese script morphology were identified. It is noticed that after T6 heat treatment, the Si particles are seen to spheroidize and fragment while the Al_2Cu phases dissolve completely. These changes lead to improved mechanical performance of the alloy.

ii. The addition of strontium increases the UTS and percentage elongation while addition of low iron and iron with manganese decreases UTS and percentage elongation in the as cast condition. T6 heat treatment increases the UTS while ductility decreases due to the fragmentation and spheroidization of Si particles.

iii. S-N fatigue tests were determined to investigate the fatigue performance of these alloys at room temperature. The results indicate that base alloy combined with strontium and base alloy showed high fatigue life (610,399 and 110,514 loading cycles respectively) as compared to base alloy with iron and base alloy combined with iron and manganese with fatigue life of 42,320 and 97,314 loading cycles. T6 heat treatment was observed to increase fatigue performance of base alloy with iron and base alloy combined with iron and manganese while T6 heat treatment was indicated to decrease fatigue performance of base alloy and base alloy with strontium.

5.2 Recommendations for Future Research

A number of further investigations on fatigue performance behavior of cast aluminium-silicon alloy for cylinder head applications should be carried out in the following areas:

i. Fatigue crack propagation behavior should be carried out to understand the effect of alloying elements on the fatigue performance of cast aluminium-silicon alloy for cylinder head.

ii. Fatigue failure analysis of secondary cast aluminium-silicon alloy under high temperature should be investigated, since cylinder heads operate under high temperature.

iii. Creep mechanism should be studied on these alloys.

iv. Effect of different heat treatment processes on the fatigue performance should be investigated.

REFERENCES

[1] J. Cui and H. J. Roven, "Recycling of automotive aluminum," *Trans. Nonferrous Met. Soc. China*, vol. 20, no. 2010, pp. 2057–2063, 2010.

[2] B. T. Kores, H. Zak, "Aluminium alloys for cylinder heads," *RMZ – Mater. Geoenvironment*, vol. 55, no. 3, pp. 307–317, 2008.

[3] Y. Birol and A. A. Ebrinç, "Critical Material Issues in Cast Aluminium Cylinder Heads," *World Foundymen Organ.*, pp. 183–188, 2008.

[4] V. Sankar, A. S. Shiva Shankare, and A. Ramesha, "Analysis of alloying elements and Mechanical properties of T6 treated Aluminium Silicon Alloys," *Int. J. Eng. Res. Technol.*, vol. 3, no. 1, pp. 515–519, 2014.

[5] S. Das, "Designing aluminum alloys for a recycle-friendly world," *Mater. Sci. Forum*, vol. 519–521, pp. 1239–1244, 2006.

[6] M. Rosso and V. T. Michel, "The influence of casting process on quality and performances on Al based automotive components," *Composites*, pp. 4–7.

[7] A. Darvishi, A. Maleki, M. . Atabaki, and M. Zargami, "The mutual effect of iron and manganese on microstructure and mechanical properties of aluminium-silicon

alloy," *Metall. J. Mater.*, vol. 16, no. 1, pp. 11–24, 2010.

[8] M. Tash, F. H. Samuel, F. Mucciardi, and H. W. Doty, "Effect of metallurgical parameters on the hardness and microstructural characterization of as-cast and heat-treated 356 and 319 aluminum alloys," *Mater. Sci. Eng. A*, vol. A443, pp. 185–201, 2007.

[9] B. K. Kosgey, S. E . Maube, D. N. Wangombe, S. M. Maranga, and J. M. Kihiu, "Effects of Additives on the Fatigue and Impact Properties of Recycled Al-Si Alloy wheels," *Sustain. Res. Innov.* 3, pp. 1–8, 2010.

[10] G. T. Zeru, B. R. Mose, and S. M. Mutuli, "The Fluidity of a Model Recycle-Friendly Al-Si Cast Alloy for Automotive Engine Cylinder Head Application," *Int. J. Eng. Res. Technol.*, vol. 3, no. 8, pp. 1504–1508, 2014.

[11] Q. Wang and P. E. Jones, "Fatigue Life Prediction in Aluminum Shape Castings," *Am. Foundry Soc.*, vol. 8, no. 3, pp. 1–20, 2013.

[12] F. B. Bahaideen, A. M. Saleem, K. M. T. Hussain, Z. M. Ripin, Z. A. Ahmad, Z. Samad, and N. A. Badarulzaman, "Fatigue Behaviour of Aluminum Alloy at Elevated Temperature," *Mod. Appl. Sci.*, vol. 3, no. 4, pp. 52–61, 2009.

[13] M. M. Yahya and N. Mallik, "Low Cycle Fatigue Failuer of Composite Materials / Aluminium Alloys At Different Heat Treatments Prossece – A review," *Int. J. Sci. Egineerind Res.*, vol. 3, no. 6, pp. 1–6, 2012.

[14] G. Zeru, “Development of Recycle-friendly Secondary Cast Aluminium Alloy for Cylinder Head Applications,” Master’s Thesis, Jomo Kenyatta University of Agriculture and Technology, Kenya, 2014.

[15] N. Nafsin and H. M. M. A. Rashed, “Effects of Copper and Magnesium on Microstructure and Hardness of Al-Cu-Mg Alloys,” *Int. J. Eng. Adv. Technol.*, vol. 2, no. 5, pp. 533–536, 2013.

[16] L. Miller, “Investigation of Thermo-Mechanical Fatigue Characteristics for Cast Aluminum (AL319-T7),” Master’s Thesis, University of Windsor, Canada, 2014.

[17] E. Ozbakir, “Development of Aluminum Alloys for Diesel-Engine,” Master’s thesis, Department of Mining and Materials Engineering, McGill University, Canada, 2008.

[18] R. S. Rana, R. Purohit, and S. Das, “Reviews on the Influences of Alloying elements on the Microstructure and Mechanical Properties of Aluminum Alloys and Aluminum Alloy Composites,” *Int. J. Sci. Res. Publ.*, vol. 2, no. 6, pp. 1–7, 2012.

[19] Y. Abdulsahib, “Effect of copper addition on the microstructure and mechanical properties of lead free solder alloy,” *Al-Qadisiya J. Eng. Sci.*, vol. 7, no. 4, pp. 366–381, 2014.

[20] J. Barresi, M. J. Kerr, H. Wang, and J. Couper, “Effect of Magnesium , Iron and

Cooling Rate on Mechanical Properties of Al-7Si-Mg Foundry Alloys," *AFS Trans.*, pp. 563–570, 2000.

[21] I. Boromei, L. Ceschini, A. Morri, A. Morri, G. Nicoletto, and E. Riva, "Influence of the solidification microstructure and porosity on the fatigue strength of Al-Si-Mg casting alloys," *Metall. Sci. Technol.*, vol. 28, no. 2, pp. 18–24, 2010.

[22] S. Fintová, R. Konečná1, and G. Nicoletto, "Microstructure, Defects and Fatigue Behavior of Cast AlSi7Mg Alloy," *Acta Metall. Slovaca*, vol. 19, no. 3, pp. 223–231, 2013.

[23] F. Stanislava, V. Konstantová, R. Konečná, and G.Nicoletto., "Experimental Study of Porosity and Fatigue Behavior af Cast Al – Si Alloys," *Metal*, vol. 13, no. 15, pp. 1–8, 2008.

[24] F. Grosselle, G. Timelli, F. Bonollo, A. Tiziani, and E. D. Corte, "Correlation between microstructure and mechanical properties of Al-Si cast alloys," *La Metall. Ital.*, no. 1, pp. 25–32, 2009.

[25] C. Castella, "Self hardening aluminum alloys for automotive applications," PhD Thesis, Porto Institutional Repository, Portugal, 2015.

[26] C. Caceres, I. Svensson, and J. Taylor, "Strength-Ductility behaviour of Al-Si-Cu-Mg Casting Alloys in T6 Temper," *International J. Cast Met.*, vol. 2003, no. 15, pp. 531–543, 2002.

[27] M. Farkašová and E. Tillová, “Modification of Al-Si-Cu cast alloy,” *FME Trans.*, vol. 41, pp. 210–215, 2013.

[28] X. Jian and Q. Han, “Formation of hypereutectic silicon particles in hypoeutectic Al-Si alloys under the influence of high-intensity ultrasonic vibration,” *Overseas Foundry*, vol. 10, no. 2, pp. 118–123, 2013.

[29] H. C. Liao, M. Zhang, J. J. Bi, K. Ding, X. Xi, and S. Q. Wu, “Eutectic Solidification in Near-eutectic Al-Si Casting Alloys,” *J. Mater. Sci. Technol.*, vol. 26, no. 12, pp. 1089–1097, 2010.

[30] H. Ye, “An Overview of the Development of Al-Si-Alloy Based Material for Engine Applications,” *J. Mater. Eng. Perform.*, vol. 12, no. 3, pp. 288–297, 2003.

[31] E. M. Elgallad, A. M. Samuel, F. H. Samuel, and H. W. Doty, “Effects of Additives on the Microstructures and Tensile Properties of a New Al-Cu Based Alloy Intended for Automotive Castings,” *AFS Trans. Am. Foundry Soc.*, vol. 118, no. 10–042, pp. 39–56, 2010.

[32] H. L. de Moraes, J. R. de Oliveira, D. C. R. Espinosa, and J. A. S. Tenório, “Removal of Iron from Molten Recycled Aluminum through Intermediate Phase Filtration,” *Mater. Trans.*, vol. 47, no. 7, pp. 1731–1736, 2006.

[33] W. Khraisat and W. A. Jadayil, “Strengthening Aluminum Scrap by Alloying with Iron,” *Jordan J. Mech. Ind. Eng.*, vol. 4, no. 3, pp. 372–376, 2010.

[34] S. Dong, S. Xiong, and B. Liu, “Numerical simulation of microporosity evolution of aluminum alloy castings,” *J. Mater. Sci. Technol.*, vol. 20, no. 1, pp. 23–26, 2004.

[35] P. Ashtari, H. Tezuka, and T. Sato, “Influence of Sr and Mn Additions on Intermetallic Compound Morphologies in Al-Si-Cu-Fe Cast Alloys,” *Mater. Trans.*, vol. 44, no. 12, pp. 2611–2616, 2003.

[36] X. Fang, G. Shao, Y. Q. Liu, and Z. Fan, “Effects of intensive forced melt convection on the mechanical properties of Fe containing Al – Si based alloys,” *Mater. Sci. Eng. A*, vol. 446, pp. 65–72, 2007.

[37] W. Zhang, B. Lin, P. Cheng, D. Zhang, and Y. Li, “Effects of Mn content on microstructures and mechanical properties of Al-5.0Cu-0.5Fe alloys prepared by squeeze casting,” *Trans. Nonferrous Met. Soc. China (English Ed.*, vol. 23, no. 6, pp. 1525–1531, 2013.

[38] D. Wang’ombe, S. Maube, S. Maranga, and J. Kihiu, “Effect of Iron-intermetallics on the Fluidity of Recycled Aluminium Silicon Cast Alloys,” *Sustain. Res. Innov.*, vol. 4, pp. 224–227, 2012.

[39] A. H. Musfirah and A. G. Jaharah, “Magnesium and Aluminum Alloys in Automotive Industry,” *J. Appl. Sci. Res.*, vol. 8, no. 9, pp. 4865–4875, 2012.

[40] M. M. Jaradeh, “The Effect of Processing Parameters and Alloy Composition on the Microstructure Formation and Quality of DC Cast Aluminium Alloys, ” PhD

Thesis, Materials Science and Engineering in KTH-Royal Institute of Technology, Stockholm, Sweden, 2006.

[41] M. Djurdjevič and M. Grzinčič, "The effect of major alloying elements on the size of secondary dendrite arm spacing in the as-Cast Al-Si-Cu alloys," *Arch. Foundry Eng.*, vol. 12, no. 1, pp. 19–24, 2012.

[42] M. Angeloni, "Fatigue life evaluation of A356 aluminium alloy used for engine cyliner head," PhD Thesis, University of Sao Paulo, Bresil, 2011.

[43] X. Zhu, "Ultrasonic Fatigue of E319 Cast Aluminium Alloy in the Long Lifetime Regime," PhD Thesis, Materials Science and Engineering in The University of Michigan, USA, 2007.

[44] R. Molina and M. Rosso, "Mechanical characterization of aluminium alloys for high temperature applications Part 2 : Al-Cu , Al-Mg alloys," *Metall. Sci. Technol.*, vol. 29, pp. 5–13, 2011.

[45] J. Lee, "Cast aluminum alloy for high temperature applications," *Miner. Met. Mater. Soc.*, 2003.

[46] Z. Kadhim, "Effect of Cooling rate on Mechanical Properties of Euctetic and Hypoeuctetic Al-Si," *J. Eng.*, vol. 17, no. 6, pp. 1576–1583, 2011.

[47] J. Pavlovic-Krstic, R. Bähr, G. Krstic, and S. Putic, "The effect of mould temperature and cooling conditions on the size of secondary dendrite arm spacing

in Al-7Si-3Cu alloy," *MJoM*, vol. 15, no. 2, pp. 105–113, 2009.

[48] L. Dobrzanski, R. Maniara, and J. H. Sokolowski, "The effect of cast Al-Si-Cu alloy solidification rate on alloy thermal characteristics," *J. Achiev. Mater. Manuf. Eng.*, vol. 17, no. 1, pp. 217–220, 2006.

[49] M. Kabir, E. Ashrafi, T. I. Minhaj, and M. Islam, "Effect of Foundry Variables on the Casting Quality of As-Cast LM25 Aluminium Alloy," *Int. J. Eng. Adv. Technol.*, vol. 3, no. 6, pp. 115–120, 2014.

[50] B. N. Sarada, P. L. Srinivasamurthy, and Swetha, "Microstructural Characteristics of Sr And Na Modified Al-Mg-Si Alloy," *Int. J. Innov. Res. Sci. Eng. Technol.*, vol. 2, no. 8, pp. 3975–3983, 2013.

[51] P. Apichai, J. Kajornchiyakul, J. T. H. Pearce, and A. Wiengmoon, "Effect of Precipitation Hardening Temperatures and Times on Microstructure , Hardness and Tensile Properties of Cast Aluminium Alloy A319," *J. Pap.*, pp. 2–7.

[52] D. Murizam and S. B. Jamaludin, "Effect of Slution Treatment Temperature on Recycled Aluminium Alloy 319," *ICoSM*, pp. 226–228, 2007.

[53] E. Sjölander, "Heat treatment of Al-Si-Cu-Mg casting alloys," Phd Thesis, Department of Mechanical Engineering, Materials and Manufacturing-Casting, School of Engineering, Jönköping University Jönköping, Sweden, 2011.

[54] S. K. Chaudhury and D. Apelian, "Fluidized bed heat treatment of cast Al alloys,"

Metall. Mater. Trans. A-, vol. 37A, no. 7, pp. 2295–2311, 2006.

[55] A. M. A. Mohamed and F. H. Samuel, "A Review on the Heat Treatment of Al-Si-Cu/Mg Casting Alloys," *Heat Treat. Nov. Appl.*, pp. 1–18, 2012.

[56] L. Hurtalová, J. Belan, E. Tillová, and M. Chalupová, "Changes in structural characteristics of hypoeutectic Al-Si cast alloy after age hardening," *Mater. Sci.*, vol. 18, no. 3, pp. 228–233, 2012.

[57] C. Van Kranenburg, Fatigue crack growth in Aluminium Alloys, PhD Thesis, Technische University Delft, Netherlands, 2010.

[58] M. Dileep, P. S. Sanjay, and R. K. Mandloi, "Analytical Study of Fatigue Failure of Aluminium Alloy Piston in IC Engines," *Int. Res. J. Eng. Technol.*, vol. 3, no. 4, pp. 1665–1669, 2016.

[59] S. Fintová, G. Anzelotti, R. KoneKonečná, and G. Nicoletto, "Casting pore characterization by x-ray computed tomography and metallography," *Arch. Mech. Eng.*, vol. LVII, no. 3, pp. 269–273, 2010.

[60] O. Kuwazuru, Y. Murata, Y. Hangai, T. Utsunomiya, S. Kitahara, and N. Yoshikawa, "X-Ray CT Inspection for Porosities and Its Effect on Fatigue of Die Cast Aluminium Alloy," *J. Solid Mech. Mater. Eng.*, vol. 2, no. 9, pp. 1220–1231, 2008.

[61] J. J. I. Mattos, A. Y. Uehara, M. Sato, and I. Ferreira, "Fatigue properties and

micromechanism of fracture of an AlSiMg0.6 cast alloy used in diesel engine cylinder head," *Procedia Eng.*, vol. 2, no. 1, pp. 759–765, 2010.

[62] J. F. Major, "Porosity Control and Fatigue Behavior in A356-T61 Aluminum Alloy," *AFS Trans.*, pp. 901–906, 2002.

[63] Q. Wang, W. Apelien, L. Arnberg, S. Gulbrandsen-Dahl, and J. Hjelen, "Porosity and Fatigue Performance Interactions in Aluminum Cast Alloys," *AFS Trans.*, pp. 249–256, 1999.

[64] S. M. Mostafavi Kashani, H. Rhodin, and S. M. A. Boutorabi, "Effects of hot isostatic pressing on the tensile properties of A356 cast alloy," *Iran. J. Mater. Sci. Eng.*, vol. 10, no. 3, pp. 54–64, 2013.

[65] H. Mayer, M. Papakyriacou, B. Zettl, and S. Vacic, "Endurance limit and threshold stress intensity of die cast magnesium and aluminium alloys at elevated temperatures," *Int. J. Fatigue*, vol. 27, no. 9, pp. 1076–1088, 2005.

[66] D. McDowell, K. Gall, M. Horstemeyer, and J. Fan, "Microstructure-based fatigue modeling of cast A356-T6 alloy," *Eng. Fract. Mech.*, vol. 70, pp. 49–80, 2003.

[67] T. O. Mbuya, I. Sinclair, A. J. Moffat, and P. A. S. Reed, "Analysis of fatigue crack initiation and S –-N response of model cast aluminium piston alloys," *Mater. Sci. Eng. A*, vol. 528, no. 24, pp. 7331–7340, 2011.

[68] P. Ljustell, “Fatigue crack growth experiments and analyses-from small scale to large scale yielding at constant and variable amplitude loading, Phd Thesis,” no. 81, p. p58, 2013.

[69] J. A. Newman, “The effects of load ratio on threshold fatigue crack growth of aluminum alloys,” PhD Thesis, In Engineering Mechanics, Faculty of the Virginia Polytechnic Institute and State University, USA, 2000.

[70] Z. Chen, P. He, and L. Chen, “The Role of Particles in Fatigue Crack Propagation of Aluminum Matrix Composites and Casting Aluminum Alloys,” *J. Mater. Sci. Technol.*, vol. 23, no. 2, pp. 213–216, 2007.

[71] D. A. Lados, D. Apelian, and J. K. Donald, “Fatigue crack growth mechanisms at the microstructure scale in Al – Si – Mg cast alloys : Mechanisms in the near-threshold regime,” *Metall. Mater. Trans. A*, vol. 37A, pp. 1475–1486, 2006.

[72] Y. Liu and S. Mahadevan, “Threshold stress intensity factor and crack growth rate prediction under mixed-mode loading,” *Eng. Fract. Mech.*, vol. 74, pp. 332–345, 2007.

[73] N. Satyanarayana and C. Sambaiah, “Fatigue Analysis of Aluminum Alloy Wheel Under Radial Load,” *Int. J. Mech. Ind. Eng.*, vol. 2, no. 1, pp. 1–6, 2012.

[74] C. Bos, G. Garagnani, and R. Tovo, “Fatigue properties of a cast aluminium alloy for rims of car wheels,” *Metall. Sci. Technol.*, pp. 3–8, 2001.

[75] M. Avalle, G. Belingardi, and M. P. Cavatorta, "Static and Fatigue Strength of a Die Cast Aluminium Alloy Under Different Feeding Conditions," *Journal of Materials Design and Applications*, vol. 216, no.1, pp. 25-30, 2002.

[76] C. J. Chen, "Optimization of Mechanical Properties in A356 via Simulation and Permanent Mold Test-Bars," PhD thesis, Department of Materials Science and Engineering, Case Western Reserve University, USA 2014.

[77] S. G. Krishna, "Effect of Strontium Modification and Heat Treatment on Microstructure of Al-319 Alloy," *Int. J. Theor. Appl. Res. Mech. Eng.*, vol. 2, no. 1, pp. 53–56, 2013.

[78] J. Peng, X. Tang, J. He, and D. Xu, "Effect of heat treatment on microstructure and tensile properties of A356 alloys," *Trans. Nonferrous Met. Soc. China*, vol. 21, pp. 1950–1956, 2011.

[79] L. Hurtalová, J. Belan, E. Tillová, and M. Chalupová, "Changes in structural characteristics of hypoeutectic Al-Si cast alloy after age hardening," *Mater. Sci.*, vol. 18, no. 3, pp. 228–233, 2012.

APPENDICES

Mechanical Properties Results

Table A 1: Variation of UTS for each alloy tested

Alloys	Condition	UTS_1	UTS_2	UTS_3	Average UTS(MPa)	S.D
BA	As casted	168.86	141.29	179.2	163.12	19.60
	H.T	226.45	218	218.1	220.85	4.85
BA+0.02%	As casted	197.12	182	155.07	178.06	21.30
	H.T	240	255	255	250.00	8.66
BA+0.38%Fe	As casted	149.92	157.87	149.9	149.9	7.98
	H.T	211.3	208.7	216.50	216.50	11.33
BA+0.9%Fe+0.45%Mn	As casted	170.58	146.46	161.05	161.05	12.83
	H.T	233.2	237.4	235.23	235.23	2.10

Table A 2: Variation in % elongation for each alloy tested

Alloys	Condition	$\%El_1$	$\%El_1$	$\%El_1$	Average $\%El_1$ (%)	S.D
BA	As casted	1.36	1.45	1.38	1.40	0.05
	H.T	0.85	1	1.2	1.02	0.18

BA+0.02%	As casted	1.75	1.62	1.63	1.67	0.07
	H.T	1.12	1	1.02	1.05	0.06
BA+0.38%Fe	As casted	1.25	0.96	1.04	1.08	0.15
	H.T	0.9	0.93	0.91	0.91	0.02
BA+0.9%Fe+0.45%Mn	As casted	1.4	1.08	1.3	1.26	0.22
	H.T	0.97	0.95	1.08	1.00	0.07